INCORPORATING SUSTAINABLE DESIGN INTO A SINGLE WELL GAS LIFT OPTIMIZATION

A Thesis

by

DAVID JOSEPH TRETIN

Submitted to the Office of Graduate and Professional Studies of
Texas A&M University
in partial fulfillment of the requirements for the degree of

MASTER OF SCIENCE

Chair of Committee,	Mahmoud El-Halwagi
Committee Members,	Maria Barrufet
	Kenneth Hall
Head of Department,	Arul Jayaraman

August 2020

Major Subject: Chemical Engineering

ABSTRACT

Gas lift is a method to increase oil production from a well using injected gas to lower the density of fluids flowing to the surface. This method is commonly used because of its effectiveness, reliability, and flexibility over a wide range of operating conditions. The gas lift process can be optimized to maximize production by controlling the rate and pressure of injected gas. Past research has focused on optimizing the gas lift operation at a single well or for many wells in the same field. Previous work has sought to optimize well production without integrating methods of sustainable design.

In this study, a well was simulated before and after gas lift was implemented to investigate the impact of the technology. The operation of the well was assumed to take place over a sufficiently short period of time such that reservoir properties and reservoir fluid composition remain constant. Production from the well was related to the bottomhole flowing pressure via an inflow performance relationship using both Darcy and Vogel models. Process simulation software (ProMax) was used to evaluate fluid properties at various conditions and to model the operation of common process units such as heat exchangers, compressors, and separators.

This study seeks to include a sustainability analysis into the design of a gas lift project. Including metrics of sustainability will quantify the tradeoffs between economics and emissions when adding gas lift to a production well. This work builds on previous work for predicting well performance, with an additional environmental consideration for evaluating project viability. A method for incorporating sustainable design is necessary for decision makers who seek to boost profitability while minimizing environmental impact.

The results of this study indicate the gas lift project would increase the profitability of the well operation and meet a common acceptable threshold for project ROI. However, if decision makers account for measures of sustainability, the project would not be profitable but costly. The conflicting directions of the economic and sustainability metrics demonstrate the need for incorporating sustainable design into project selection.

ACKNOWLEDGMENTS

I would like to say thank you to my academic advisor, Dr. Mahmoud El-Halwagi for his help and support throughout my graduate studies. His feedback and guidance helped encourage me and gave me confidence in my work. I also wish to thank my committee members Dr. Kenneth Hall and Dr. Maria Barrufet for their help and contribution to this work.

I could not have completed this work without the support of my colleagues at Bryan Research & Engineering and my employer, Dr. Jerry Bullin, who encouraged me to pursue a graduate degree. The expertise at BR&E provided me with a valuable and accessible source of knowledge on process simulation and design.

I am thankful to my classmates and friends at Texas A&M with whom I studied in graduate school including my roommate Andrew Palughi and coworker Mathew Derichsweiler. My research and graduate career would not have been possible without the support of the faculty and staff in the Chemical Engineering Department at A&M.

Finally, I am thankful for the love and encouragement of my family and friends who always believed in me. My parents and brothers helped me to overcome many obstacles on this journey. I also wish to thank my fiancée and future wife, Victoria White, for her love and support.

CONTRIBUTORS AND FUNDING SOURCES

Contributors

This work was supported by a thesis committee consisting of Professor Mahmoud El-Halwagi and Dr. Kenneth Hall of the Department of Chemical Engineering and Professor Maria Barrufet of the Department of Petroleum Engineering.

All work conducted for the thesis was completed by the student independently.

Funding Sources

This research was funded in part by Bryan Research & Engineering, LLC.

NOMENCLATURE

AEP	Annual Net Economic Profit
ASP	Annual Sustainability Profit
CEPCI	Chemical Engineering Plant Cost Index
EIA	Energy Information Administration
EOR	Enhanced Oil Recovery
EOS	Equation of State
FCI	Fixed Capital Investment
GOR	Gas Oil Ratio
GPSA	Gas Processors Suppliers Association
IPR	Inflow Performance Relationship
IROI	Incremental Return on Investment
ISWROIM	Incremental Sustainability Weighted Return on Investment Metric
MSCFD	Thousand Standard Cubic Feet per Day
MTPA	Metric Tonnes Per Annum
NPV	Net Present Value
OIP	Oil in Place
PVT	Pressure-Volume-Temperature
ROI	Return on Investment
SWROIM	Sustainability Weighted Return on Investment Metric
TCI	Total Capital Investment
VRU	Vapor Recovery Unit
WCI	Working Capital Investment

TABLE OF CONTENTS

Page

LIST OF FIGURES

FIGURE Page

LIST OF TABLES

TABLE Page

1. INTRODUCTION

The continued growth of the global population and economies of the world inevitably increases demand for energy production. The United States, in particular, meets its energy demands through a variety of sources as shown in Figure 1.1. The largest source of energy consumed in the US given in Figure 1.1 is petroleum followed closely by natural gas (EIA, 2019). In 2018, according to the Energy Information Administration (EIA) the US consumed 36.9 and 31 quadrillion BTU in energy from petroleum and natural gas, respectively, and these numbers are only expected to increase. Producers of these fossil fuels must continually work to extract oil and gas with ever-increasing efficiency to prolong the energy reserves of the planet and bolster production. Petroleum is formed from organic material exposed to high pressures and temperatures beneath the surface of the earth. Porous rock formations trap the hydrocarbons underground in natural reservoirs, and wells are drilled into the reservoirs from the surface to extract the resources.

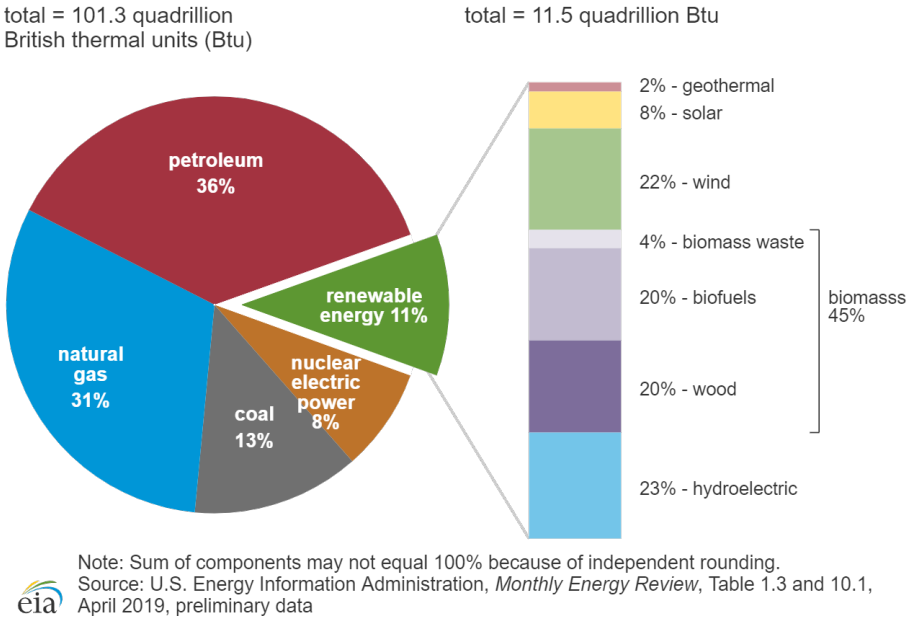

Figure 1.1: Reprinted from EIA, 2019: US Primary Energy Consumption by Energy Source, 2018

Petroleum fluids are produced from a reservoir when a pressure differential occurs at the face of the reservoir to transport fluids into the well and to the surface. The typical life cycle of an oil and gas well includes a number of stages of production which are broken down by mode of recovery. Typical production stages, their respective recovery fractions, and common methods are given in Table 1.1. Primary production refers to oil and gas extracted by the natural source of energy or drive in the reservoir. Natural drive can occur due to oil and gas expansion, vapor liberation, encroachment of nearby water sources, such as aquifers, oil drainage due to gravity, and formation consolidation. Primary recovery production usually results in the extraction of 20 to 25% of the oil in place (OIP). Over time, the production of fluids from the reservoir will decrease the reservoir pressure, and the resulting diminishment in pressure drop at the bottom of the well will decrease production. At this point additional intervention is required to continue producing from the well.

The second stage of production occurs when a well has exhausted the natural drive in the reservoir. Secondary recovery involves injecting fluids such as water or immiscible gas to maintain the reservoir pressure. Injection of water or gas also displaces hydrocarbons in the reservoir in the direction of the well. The end of secondary production is marked by considerable recovery of the injected fluids which leads to economically unfavorable operation of the well.

Tertiary production of the oil reservoir uses enhanced oil recovery (EOR) methods to further produce hydrocarbons through the well. EOR processes are commonly classified as thermal, chemical, and miscible floods. All EOR methods use an external source of energy to further produce from the reservoir. Thermal recovery is one of the most common type of EOR in the US and involves heating the oil to allow it to flow more easily. These methods typically inject steam into the reservoir to heat the oil or even burn a portion of the oil for heating purposes. The least common form of EOR is chemical recovery, which is achieved by applying chemical solutions to the reservoir to reduce the surface tension between the oil and water. Miscible gas flooding introduces a gas, such as carbon dioxide or nitrogen, which mixes with the oil to change its properties. The miscible gas can reduce the surface tension between the oil and water or reduces the viscosity of the oil allowing it to flow more freely. EOR methods are different from secondary recovery meth-

ods because they attempt to change physical properties of the oil to boost production. The ultimate recovery from each particular well around the world can vary significantly, but estimates are given in Table 1.1.

Production Type	**Typical Recovery (%)**	**Methods**
Primary	20-25	Natural drive
Secondary	15-25	Injection of gas or water
Tertiary	20-40	Enhanced oil recovery

Table 1.1: Production Stages of Conventional Oil Reservoirs

A range of artificial lift methods can also be used at any production stage to manage bottomhole pressure and other changes in conditions as the reservoir produces fluids. Artificial lift can include gas lift, rod pumping, electric submersible pumping, and others. If a well is actively flowing, it may either use gas lift or no artificial lift. When gas lift is applied to a low-producing well, natural gas is injected at high pressure into the annular space between the casing and production tubing. The high-pressure gas mixes with fluids produced by the reservoir, lowering the density. With a lower density, the hydrostatic head in the well is lowered which leads to a decrease in the bottomhole pressure. As the production from the reservoir is determined by the pressure drop at the sandface of the reservoir, a decrease in bottomhole pressure increases production. Figure 1.2 indicates the location of the bottomhole pressure, p_{wf}, the pressure at the sandface, p_{wfs}, and the average reservoir pressure, p_R. Gas lift is often used because it is effective over a range of operating conditions, simple to install, and robust in operation. One potential drawback to using gas lift is the need for a steady stream of lift gas which is not always available.

One difficulty associated with using gas lift in a well is the determination of an appropriate injection rate and pressure. The rate of injected gas determines the volume of liquids which can

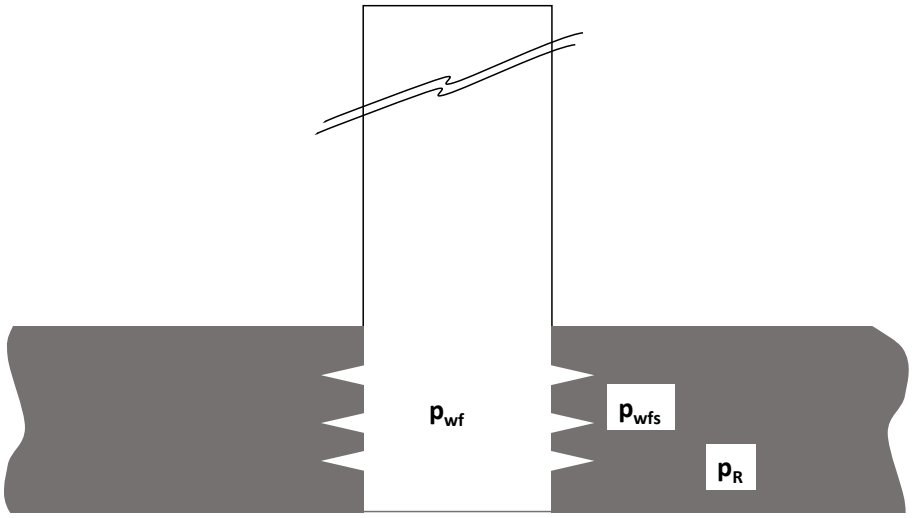

Figure 1.2: Relevant Pressures in a Well and Reservoir

be brought to the surface and can have a large impact on the pressure losses in the wellbore and elsewhere in the facility. When the injection rate of lift gas is increased, the recycled gas makes up a larger portion of produced fluids. More gas in the wellbore also leads to an increased fluid velocity and associated pressure drop in the tubing. Therefore, a balance must be struck between the lifting effect and pressure drop with injected gas to optimize production. A single well optimization seeks to maximize production from a well given the current and future reservoir conditions, well size, depth, temperature profile, and surface equipment constraints.

The problem of gas lift optimization can be expanded by considering an entire gathering network with many wells producing variable gas oil ratios (GOR). To optimize production of a gathering system, all collected natural gas must be allocated to each of the wells to maximize production. If a limitless supply of lift gas were available, the optimal amount of gas could be supplied to each well to maximize global production. However, available gas is usually not sufficient to supply all wells optimally. To solve the network gas lift problem, the allocation is considered as a maximization problem of a nonlinear function. The function models total oil production for the field subject to physical constraints. A curve, known as the gas-lift performance curve (GPLC), is generated by plotting the oil production rate vs the gas injection rate either by direct measurement or by

computer simulation. Variables which determine the nonlinear function include the gas injection rates for each well. Various optimization techniques have been used in the literature to solve this nonlinear optimization problem (Alarcón et al., 2002).

Gas lift optimization, either single well or network-based, typically does not account for the number and depth of gas lift valves. This is because the configuration of the well is complete by the time it is producing and is not considered to be variable. However, the problem of redesigning the well has been considered in the literature for a workover scenario of an individual well to boost production.

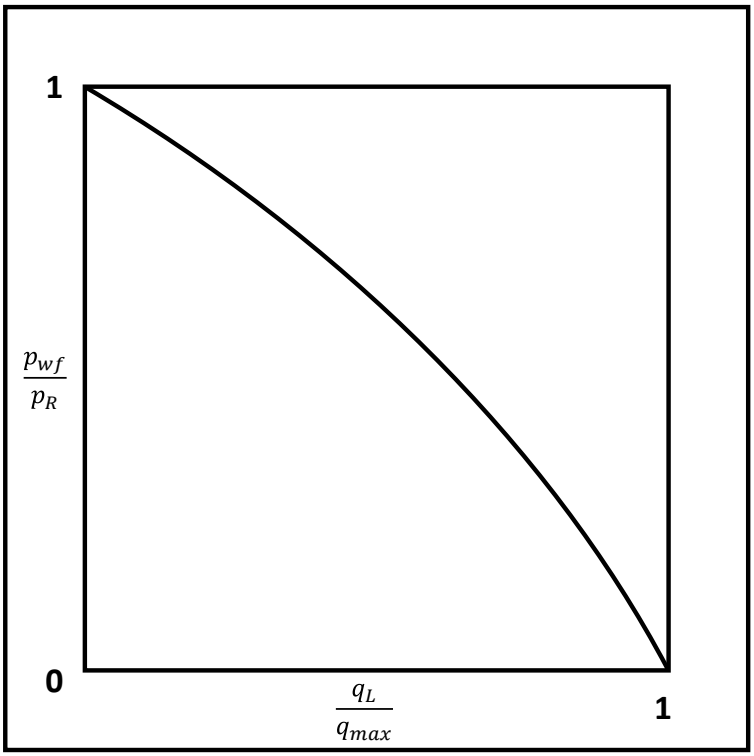

Figure 1.3: IPR Example Plot

Optimizing the performance of a well also requires accurate modeling of the petroleum reservoir to predict production as a function of bottomhole pressure. This relationship is known as an inflow performance relationship (IPR), and the data required to create an IPR are collected by mea-

suring production rates from the well at different drawdown pressures. From a physical standpoint, the shape of the IPR curve is determined by the composition and behavior of the produced fluids. A typical IPR curve is given in Figure 1.3. The figure plots dimensionless pressure vs dimensionless flow. The pressure ratio varies linearly at lower flow rates before quickly approaching zero at the maximum flow rate.

A common assumption made in creating an IPR is a fixed average reservoir pressure, p_R. The pressure drop at the sandface, a porous interface between the reservoir and wellbore, can have a complex relationship with the flow into the well depending on the properties of the rock, flow regime, compressibility, composition, drive mechanism, damage to the formation, or stimulation (Beggs, 1991). The pressure drop in a reservoir can be calculated using an equation for pressure drop due to viscous shear force as a function of flow. This relationship can take different forms depending on application, but all forms are based on Darcy's law. The differential form of Darcy's law for linear flow is given in Equation 1.1 in terms of fluid velocity and the integral form is given in Equation 1.2 in terms of volumetric flow rate (Darcy, 1856).

$$\nu = \frac{k\ dp}{\mu\ dx} \tag{1.1}$$

$$q = \frac{CkA(p_1 - p_2)}{\mu L} \tag{1.2}$$

Where:

A = surface area,

C = unit conversion factor,

k = permeability,

L = length over which pressure drop occurs,

μ = fluid viscosity,

ν = fluid velocity,

p = pressure,

q = volumetric flow rate,

x = distance

Darcy's equation can also be rewritten for radial flow and integrated to give the flow rate as a function of pressure drop and radial parameters of the well and reservoir. Oils are assumed to be slightly compressible, which is accounted for with an oil formation volume factor, B_o. To integrate Darcy's equation for gases, the product of density and flow rate, ρq (mass flow), is assumed to be constant, and the gas equation of state (EOS) is used to relate the pressure, p, and density, ρ. The integrated form of Darcy's equation for gas gives the flow rate in terms of permeability, average reservoir pressure, wellbore flowing pressure, gas viscosity, reservoir temperature, and other properties of the reservoir and produced fluids. Oftentimes, the integral forms of the Darcy equation for oil and gas are rearranged to give the flow rate as a function of the pressure drop multiplied by a combined term known as the productivity index, J, as given in Equation 1.3.

$$q_0 = J(p_R - p_{wf}) \tag{1.3}$$

The variable p_R refers to the average reservoir pressure, and p_{wf} is the wellbore flowing pressure. The productivity index concept can be useful because if a well is operating such that J is constant, it can be used to predict inflow for future operation once it has been calculated. Of course, it is seldom the case that J is constant and can be affected by many factors including the phase behavior in the reservoir, such as if gas is being liberated; the relative permeability behavior, which can change for an oil depending on gas saturation levels; the oil viscosity behavior, which is dependent on gas saturation, temperature, and pressure; and the oil formation volume behavior, which is defined as the ratio of the volume of oil with dissolved gas over the volume of oil at stock tank conditions.

The Darcy equation and its application to oil and gas flow could be used if all the parameters were known, but, unfortunately, this is rarely the case. Therefore, the IPR is not commonly estimated via the Darcy equation. Instead, empirical methods are used to predict inflow performance which usually require at least one stabilized test on the well. These empirical methods include the Vogel method, the Fetkovich method, and the Jones, Blount and Glaze method which will be presented below.

The Vogel method is based on a mathematical study on 21 widely different reservoir conditions with varying oil, permeability, well spacing, and skin factor characteristics. The method has been found to be applicable to any reservoir for which gas saturation increases with decreasing pressure (Vogel, 1968). Vogel's method includes a dimensionless pressure, p_{wf}/p_R, and a dimensionless flow rate, $q_0/q_{0(max)}$, which is the flow rate at the well pressure considered, p_{wf}, divided by the maximum theoretical flow rate which would occur at zero wellbore pressure. Vogel found the IPR curves at various operating conditions have the same general shape that can be described by Equation 1.4 with variables defined previously.

$$\frac{q_0}{q_{0(max)}} = 1 - 0.2\left(\frac{p_{wf}}{p_R}\right) - 0.8\left(\frac{p_{wf}}{p_R}\right)^2 \tag{1.4}$$

The method proposed by Fetkovich for predicting inflow performance used the same type of equation previously used to examine gas well performance. Fetkovich's model was found to predict reservoir performance for a wide range of permeability values and saturation levels (Fetkovich, 1973). Equation 1.5 gives the general form given by Fetkovich, where C is a flow coefficient and n is an exponent which depends on the characteristics of the well. Use of the Fetkovich method requires a minimum of two well tests to determine C and n, but, traditionally, at least four tests are conducted to reduce any error in the data.

$$q_0 = C\left(p_R^2 - p_{wf}^2\right)^n \tag{1.5}$$

Jones et al. (1976) expanded on the productivity index equation (1.3) to include the effects of

turbulence or non-Darcy flow in the IPR model. Equation 1.6 gives the Jones, Blount, and Glaze equation which defines the pressure drop in the well as a function of the production rate, where A and B are grouped parameters, which can be calculated or estimated from known values. The Aq_0 term accounts for pressure difference due to laminar flow, and the Bq_0^2 term accounts for turbulent flow.

$$p_R - p_{wf} = Aq_0 + Bq_0^2 \tag{1.6}$$

This work presents an economic and sustainability assessment of a gas lift process in a simulated well. The sustainability analysis accounts for environmental impact which is predicted to occur if the project it implemented. Previous work has assessed gas lift projects from an economic profitability standpoint, whereas, this work will extend the profitability analysis with metrics of sustainability. This augmented project assessment addresses a growing interest in sustainable design among decision makers.

The well will be simulated alone to give a baseline for comparison. The base case will be compared to a case which applies recycled natural gas as lift gas. The injection rate and pressure of lift gas will be optimized, and the optimized case will be compared to the base case production rate. Both cases will be simulated using ProMax, which is a process simulation software developed by Bryan Research and Engineering in Bryan, Texas. The simulation software will incorporate the Darcy model to produce an IPR for modeling the production of reservoir fluids as a function of bottomhole pressure. ProMax also has built-in correlations for multiphase flow which will be used to model the oil and gas flow in the production tubing. The software can simulate the thermodynamic properties of fluids using a number of equations of state (EOS) to predict the properties of fluids in the production system.

An economic analysis will also be performed to demonstrate the benefits of using gas lift. The economic analysis will be conducted in the context of sustainability in process improvement using metrics introduced by El-Halwagi (2017) including annual sustainability profit (ASP) and incremental sustainability weighted return on investment metric (ISWROIM).

The profitability of a project is often determined using the return on investment (ROI) which is defined in Equation 1.7. ROI is calculated by dividing the annual net economic profit (AEP) by the total capital investment (TCI). The concept of ROI can be extended to projects which are incremental in nature with an incremental return on investment (IROI) given in Equation 1.8. IROI is found by dividing the change in AEP by the change in TCI. A project is considered economically viable if its ROI or IROI meets a minimum threshold set by the company.

$$ROI = \frac{AEP}{TCI} \tag{1.7}$$

$$ROI = \frac{\Delta AEP}{\Delta TCI} \tag{1.8}$$

El-Halwagi extended the concept of ROI to incorporate sustainability into the design of new and incremental project design. The new metric introduced, sustainability weighted return on investment metric (SWROIM), replaces the AEP term with a term representing the annual sustainability profit. This term accounts for sustainability metrics which a company seeks to simultaneously maximize. ASP is given in Equation 1.9 and defined by El-Halwagi to be the weighted sum of economic and sustainability factors.

$$ASP = AEP\left[1 + \sum_{i=1}^{N_{indicators}} w_i \left(\frac{Indicator_i}{Indicator_i^{Target}}\right)\right] \tag{1.9}$$

In Equation 1.9, the index i counts the number of different sustainability indicators and w_i is a weighting factor for the ratio of relative importance of the indicator compared to new economic profit. The addition of one in the equation gives a baseline as the net economic profit and serves as the basis for sustainability indicators. The numerator of the indicator ratio, $Indicator_i$, is the value of the sustainability indicator, and the denominator, $Indicator_i^{target}$, is a target for that indicator. The indicator target can be a benchmark set by the company or a maximum value from all considered projects. ASP can be thought of as an extended form of AEP which accounts for the sustainability targets the project is attempting to meet. ASP also replaces AEP in the SWROIM

metric given in Equation 1.10 which is analogous to ROI.

$$SWROIM = \frac{ASP}{TCI} \tag{1.10}$$

$$ISWROIM = \frac{\Delta ASP}{\Delta TCI} \tag{1.11}$$

Similar to ROI, the metric SWROIM can also be used for an incremental project by replacing ASP and TCI with incremental values resulting from implementation of the project. The incremental version, ISWROIM, is given in Equation 1.11 and is analogous to IROI with an accounting for sustainability indicators. Metrics accounting for sustainability give companies and design engineers tools to quantify and reconcile aspects of a project which go beyond merely economic value. Weighting values also provide a means for adjusting relevant indicators along with the changing needs of the company.

2. LITERATURE REVIEW

Artificial lift systems are used to stimulate or improve production from a well. A number of methods can be used depending on the conditions of the well and the desired production. An overview of artificial lift methods is given by Brown (1982). The paper discusses advantages and disadvantages of gas lift which include flexibility, high volume, and remotely powered as opposed to, inefficiency for small wells, difficulty handling emulsions, and safety concerns due to high pressure (Brown, 1982).

A review and history of gas lift methods is given by Osuji (1994). This paper gives a simple overview of the gas lift process and some of the motivations for choosing this method of artificial lift. Osuji also describes the development of gas lift systems from the first practical application which occurred in 1846 (Osuji, 1994).

A common method for well production optimization is NODAL™ Analysis which is described by Beggs (1991). NODAL™ Analysis is commonly used to model the production of a single well and can handle either black oil or compositional fluid descriptions. The model is also used to predict multiphase flow behavior during production (Beggs, 1991).

Using NODAL™ Analysis, a production optimization can be carried out on a single well or on a field of wells using gas lift. Single well optimizations are oftentimes incomplete because they do not take into account the potential influence of one well on another, but they do provide a model which can be extended to a network optimization problem.

An example of a single well optimization using NODAL™ Analysis is given by Denney (2002). The optimization is carried out on a horizontal well with gas lift. Denney constructs a gas lift performance curve, and he uses NODAL™ Analysis to determine production rate, valve spacing, injection depth, injection volume, and wellhead pressure (Denney, 2002).

Another single well optimization method was by Vázquez-Román and Palafox (2005). They argue that other gas lift optimization methods overly simplify the problem, and, instead, they formulate a model based on mass, energy, and momentum balances. The model also uses cubic

equations of state to estimate thermodynamic properties and phase equilibrium properties. The paper argues that more accurate results are produced for both optimization and simulation of gas lifted wells (Vázquez-Román and Palafox, 2005).

Dutta-Roy and Kattapuram presented a NODAL™ Analysis for a single well using gas lift and described the performance in terms of a balance between improved buoyancy in the tubing and increased back pressure in the flow line. They then extended the analysis to two wells sharing a common flow line and investigated how the production of one well influences the other. When extended to an interconnected network of wells using gas lift, the authors argue that simple single well analyses cannot adequately be extended for purposes of optimization (Dutta-Roy and Kattapuram, 1997).

A field optimization of gas lift wells was carried out by Redden et al. (1974). The distribution of available lift gas was determined by the contribution of each well to overall production. Redden used this method of optimization to distribute lift gas to 1500 wells in a Venezuelan field. The procedure optimized the overall production at the expense of individual well production if necessary (Redden et al., 1974).

The formulation of an economic slope relating liquid production and gas injection to cost and profit was discussed by Kanu et al. (1981). This method attempts to solve the problem of gas allocation in a field with limited lift gas. The idea behind the curve is that the additional profit from additional recovery of oil must be equal to or greater than the additional cost of the injected gas (Kanu et al., 1981).

Mora et al. (2005) took a holistic approach to gas lift optimization which included modeling the reservoir, wells, surface facility, and economics to maximize net present value (NPV). The optimization was carried out by integrating mathematical models describing the behavior of the reservoir, fluids, and predicted future economic performance of the field. The authors argue that their optimization method produces different results from those which seek to optimize gas lift efficiency of single wells or overall field production rate (Mora et al., 2005).

Previous work has approached the problem of gas lift optimization using a strictly financial

profitability evaluation. Profitability provide a means for assessing the relevant strengths and weaknesses of alternate projects. This work incorporates previous methods for modeling a gas lifted well while also integrating metrics of sustainability for evaluating the overall impact of the project. The use of a sustainability analysis in this work highlights the need for such metrics in cases where profitability is increased at the expense of environmental impact.

3. PROBLEM STATEMENT AND APPROACH

3.1 Problem Statement

As mentioned previously, one common method of recovery is reinjection of natural gas into a low-producing well. The gas is injected at high pressure through the annulus to mix with the produced fluids near the reservoir. This process lowers the effective density of produced fluids and the hydrostatic pressure in the well. Reduction in pressure at the sandface increases the pressure differential at the reservoir interface and increases the driving force for production.

As the injection rate is increased, the fluid velocity and friction losses also increase until they overcome the losses in hydrostatic pressure. The relationship between injected gas rate and production can be visualized with a plot such as the example given in Figure 3.1. From the plot of produced liquids vs injected gas, an optimum can be selected based on economic value. The aim of this study is to investigate the optimum recycle rate for a single well.

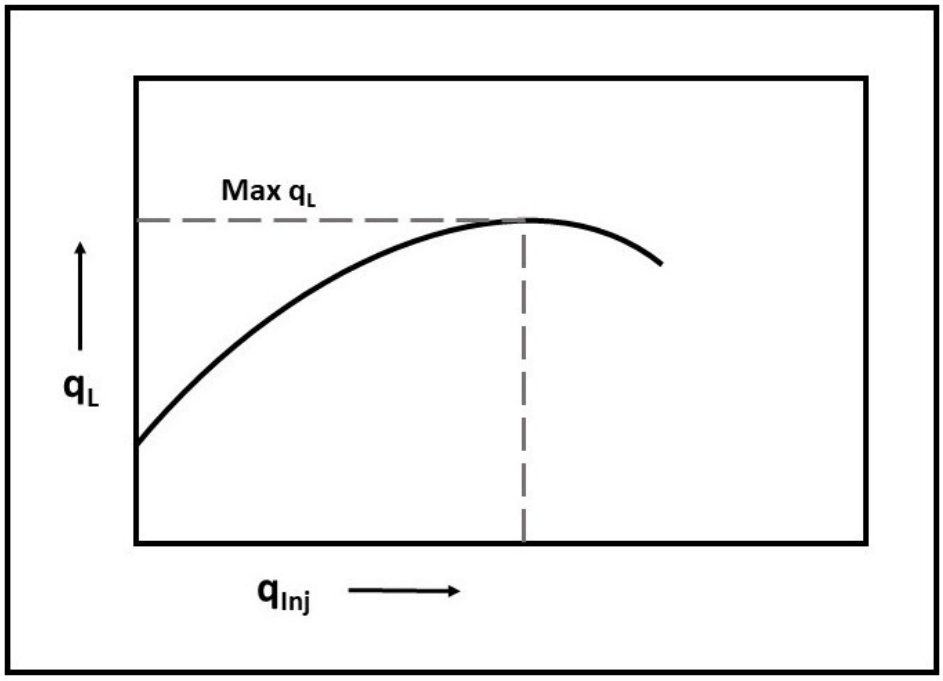

Figure 3.1: Gas Injection vs Liquid Rate

This study is conducted on a well with a given reservoir fluid composition and single well test. The well test produced 1200 bbl/d at a bottomhole pressure of 3200 psia. Equipment specifications are given for both the base case and lift gas project. It is desired to identify the optimal re-injection rate of natural gas that will optimize the production profitability as evaluated by increased production. It is also desired to investigate the tradeoffs between economic and sustainability metrics in optimizing the well performance. These tradeoffs will provide an additional dimension for consideration when deciding whether to implement the gas lift project.

3.2 Approach

First, a single well will be simulated using ProMax without recycle as described in the process description section. Appropriate thermodynamic and fluid dynamic correlations will be used to model the process as a base case. The base case will establish the performance of the well without artificial lift. Next, a recycle stream will be added to reinject produced gas into the well. The recycle flow rate will be optimized to maximize economic value, and this optimum case will be compared to the base case without recycle.

After the base and optimum cases have been simulated and compared, the benefits and drawbacks of employing gas lift in the well will be examined. An economic analysis will also be performed on the two cases to determine the relative impact of gas lift on the system economics. This economic analysis will only examine operating costs and assumes the necessary capital equipment is available for use at the well site.

Finally, a production curve will be constructed by evaluating the model for a range of recycle rates and measuring the corresponding liquids production. This production curve is expected to first increase with increasing gas injection before decreasing as frictional losses become more significant in the tubing. This production curve will shift over time, as the reservoir is depleted and must be updated accordingly.

The flowchart representing the simulation and analysis process for the entire thesis is given in Figure 3.2. The two cases will be simulated in parallel and are independent of one another.

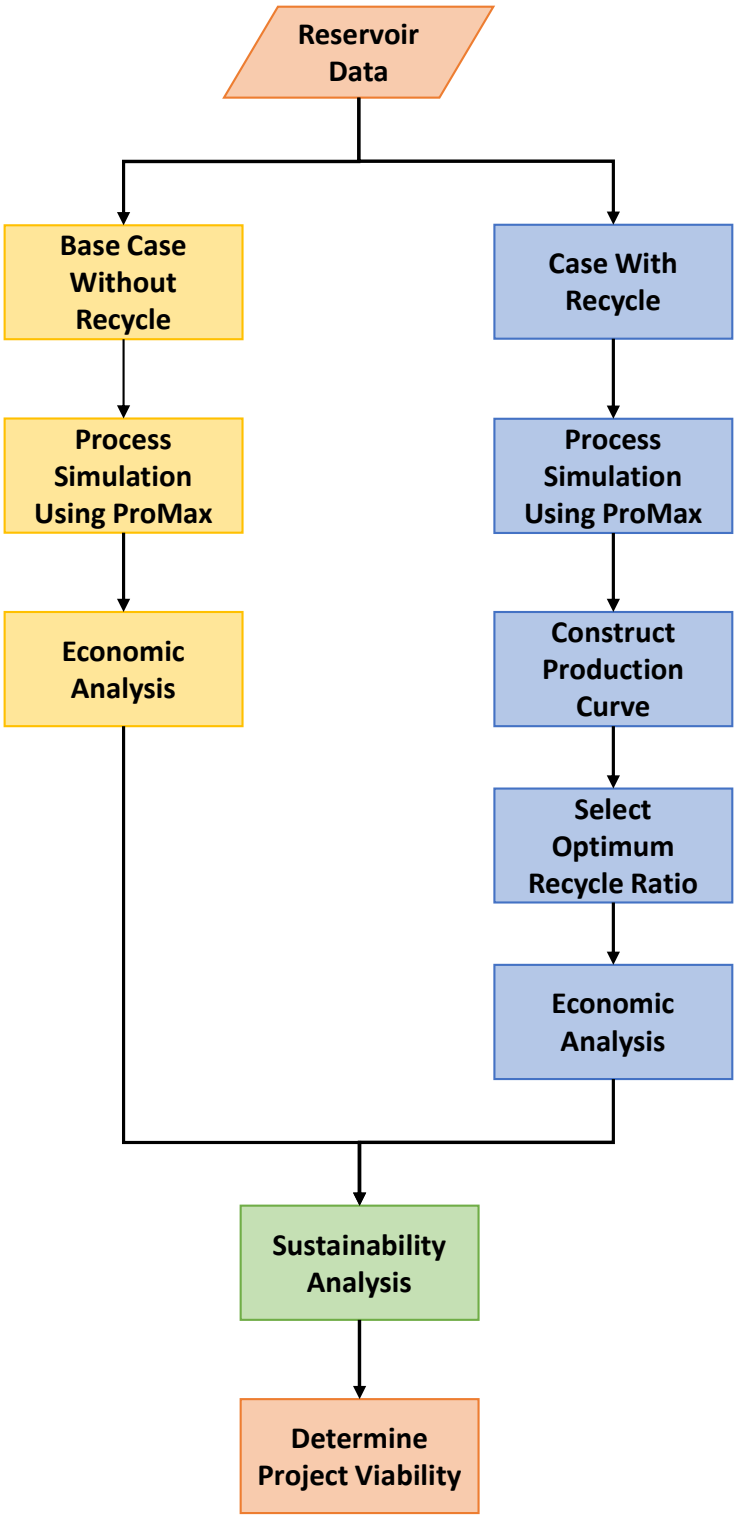

Figure 3.2: Approach Flowchart

3.3 Process Description

A detailed description of the process elements used in the facility model are given in this section. The process examined by this work consists of a reservoir from which oil flows; production tubing which connects the reservoir to the surface; surface equipment consisting of the wellhead, choke and surface flowline; and the production separator. Well production at a facility like the one modeled typically produces oil, gas, and water which all flow up from the reservoir. The driving force behind the upward flow can either be the reservoir pressure or some form of artificial lift. A schematic of the production facility without recycle is given in Figure 3.3.

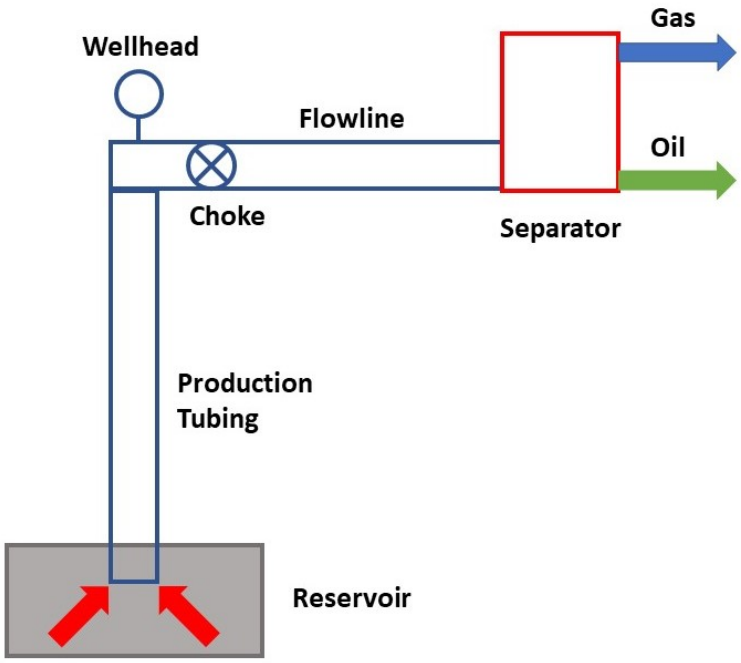

Figure 3.3: Overview of a Production Facility

A petroleum reservoir is a naturally occurring pool of hydrocarbons beneath the surface of the earth. Reservoirs can be classified as either conventional or unconventional. Hydrocarbons - either oil or natural gas - in a conventional reservoir are sealed in by a capping rock formation with low

permeability. Alternatively, unconventional reservoirs have surrounding rock with high porosity and low permeability. Unconventional reservoirs do not require a cap rock.

A key factor that influences the characteristics of a reservoir is depth. Deeper formations tend to be more compacted and consolidated. Depth can also influence permeability and porosity. Shallow reservoirs are far more permeable than deep reservoirs. For reference, permeability at 3,000 ft can be measured to be in excess of 10,000 md, while reservoirs at a depth of 20,000 ft commonly measure permeability to be 0.1 md or less. The porosity of a reservoir follows a similar trend with deeper formations exhibiting higher porosity (Wang and Economides, 2009).

A producing reservoir goes through five phases during its life:

i. Exploration

ii. Discovery

iii. Appraisal and Delineation

iv. Development

v. Production and Abandonment

Exploration of petroleum plays marks the beginning of a reservoir's production life. A petroleum play is a geological structure which may indicate the presence of hydrocarbon accumulation. A play then becomes a prospect as evidence points to the mounting possibility of an oil and gas presence. A reservoir is discovered when exploratory wells successfully strike them.

The next step is to drill an appraisal well which is used to evaluate the reservoir. An appraisal well seeks to determine the size and quality of a reservoir and determine whether it meets the standard for production. The reservoir is then developed by drilling oil and gas wells for optimal production. Next, the reservoir is produced to bring the hydrocarbons to the surface. The initial production is driven by a primary drive which is energy stored naturally in the reservoir (Satter and Iqbal, 2016). Such natural energy includes:

i. Oil and Gas Expansion

ii. Vapor Liberation

iii. Encroachment of Nearby Water Sources

iv. Oil Drainage

v. Formation Consolidation

After primary drives are exhausted, the well can be further produced using secondary drive measures. Secondary or recovery drives commonly used include injected water or gas to displace oil and maintain the reservoir pressure. Tertiary recovery or enhanced oil recovery can then be employed to continue production. EOR methods can be broken down into thermal, chemical, and miscible gas. Historically, the lifetime recovery of a typical oil reservoir is 25-50%. Finally, as a reservoir no longer produces at an economical level, it is abandoned (Satter and Iqbal, 2016).

After a suitable oil reservoir has been discovered and appraised, it is produced by drilling an oil or gas well. The wellbore is lined with casing to protect layers of soil and any underground water sources such as aquifers. The casing prevents contamination and stabilizes the well during the production phase. The casing has 4.5 or 5.5 in diameter, as it fits just inside the wellbore. This diameter is too wide to optimally produce from the well as the reservoir pressure declines. To solve this problem, production tubing is used which has a narrower diameter. The tubing transports oil and gas from the reservoir to the surface.

Selection of an appropriate tubing size is critical to optimize well production. For example, a well that produces both gas and liquids depends on the gas to lift liquids to the surface. Tubing that is too narrow increases friction losses and results in a greater pressure drop. As the tubing size is increased, friction losses decrease, resulting in a lower bottomhole pressure. The decreased bottomhole pressure, in turn, increases the inflow from the reservoir. As tubing size is further increased liquid loads the well and reduces gas velocity. After well completion, the casing size cannot be changed, but tubing size may be adjusted during a workover to boost production if it is limiting the operation of the well.

The surface equipment is made up of all the equipment at the production facility between the tubing and the separator. All surface equipment has an associated pressure drop which must be accounted for when modeling the production facility. First, the wellhead marks the top of the wellbore and provides an interface for insertion and removal of production equipment. The wellhead also serves as a point of suspension and pressure seal for casing and tubing.

Next, a choke valve is used to control the fluid flow from the well. The valve also regulates downstream pressure by flowing fluid through a small valve opening. Choke valves also protect surface equipment from erosion and slugging over the course of well production. A choke placed at the wellhead fixes the wellhead pressure. The fixed wellhead pressure also fixes the bottomhole pressure and production rate if the pressure losses in the tubing remain constant.

Finally, the flowline is simply a run of pipe connecting the wellhead and choke to the surface separator. Depending on the setup of the well site and the location of the separator, the flowline can have different lengths and, thus, different pressure drops for a given flow.

The production separator is a large pressure vessel used to separate the well stream fluid into oil, gas, and water. A separator pressure is set based on the ratio of oil and gas that will produce the greatest economic value. When using gas lift with recycled gas, the separator must have a large enough capacity to handle the formation gas along with the injected lift gas. It is also important to operate the separator at a sufficiently low pressure to maximize available lift gas.

4. METHODOLOGY

The major work of this thesis consists of simulation of a well with and without gas lift from recycle; development of an IPR model for predicting the reservoir production; and application of sustainability parameters for comparison of the two simulations. The major pieces of process equipment are modeled using ProMax. The software includes a feature for implementing user-defined expressions which incorporate the IPR model based on Darcy's equation. The data from the simulation is also used to draw comparisons between the base and recycle cases. Finally, sustainability parameters are determined using results of the simulation according to the relationships previously defined.

4.1 Base Case

The gas lift process was designed and modeled in the process simulator software ProMax version 5.0. ProMax is commonly used by engineers to design and optimize simulated chemical processes, such as gas processing and refining. The software uses thermodynamic and fluid dynamic models to calculate properties of fluids at given conditions. ProMax was used to construct a flowsheet from the process flow diagram given in Figure 4.1. The simulation flowsheets are given in the Appendix and include an inlet stream for the reservoir; piping sections for the production tubing and surface line; a valve for the wellhead and choke; a separator to model the surface separator; and compressors, heat exchangers, and separators to model a three stage compression station for the recycled lift gas.

In the simulation software, the Peng-Robinson property package was selected which uses the Peng-Robinson EOS to model both vapor and liquid phases in the flowsheet. This predefined property package is suitable for modeling light or heavy hydrocarbon systems without polar components, making it suitable for modeling this system. The property package calculates the phase equilibrium when multiple phases are present in a single stream. All material and energy balances are handled by the model and the various unit operations in the flowsheet. ProMax is a steady-state

simulation software, therefore, the gas lift process and reservoir are assumed to be at steady state.

The pressure-volume-temperature (PVT) analyses for several wells were provided by Dr. Maria Barrufet for offshore wells located in the Gulf of Mexico, off the coast of Louisiana. The compositions of the reservoir fluids for these wells are given in Table 4.1 which shows a variety of possible fluid compositions. It is important to note the last component in the table, C_{7+}, is a lumped component which combines all components with seven carbon atoms or more into one. The C_{7+} component can have different properties depending on its constituent components, so the PVT analysis includes molecular weight and specific gravity measurements for this component for characterization. The composition from Well 6 will be used to model the reservoir fluid in this study.

Component	**Well 1**	**Well 2**	**Well 3**	**Well 4**	**Well 5**	**Well 6**
N_2	0.18	0.21	0.19	0.07	0.14	0.60
CO_2	0.08	0.06	0.09	0.02	2.82	0.14
C_1	97.18	83.81	73.78	53.29	81.06	39.21
C_2	0.96	3.94	5.45	1.61	3.97	7.15
C_3	0.43	2.20	3.29	1.27	2.09	6.02
iC_4	0.13	0.51	0.75	0.35	0.83	1.23
nC_4	0.19	0.89	1.47	0.65	0.60	3.49
iC_5	0.09	0.41	0.66	0.26	0.35	1.46
nC_5	0.08	0.45	0.77	0.30	0.27	1.95
C_6	0.13	0.76	1.23	0.68	0.51	3.02
C_{7+}	0.55	6.76	12.32	41.50	7.36	35.73

Table 4.1: Compositions of Reservoir Fluids from Different Wells in Mole %

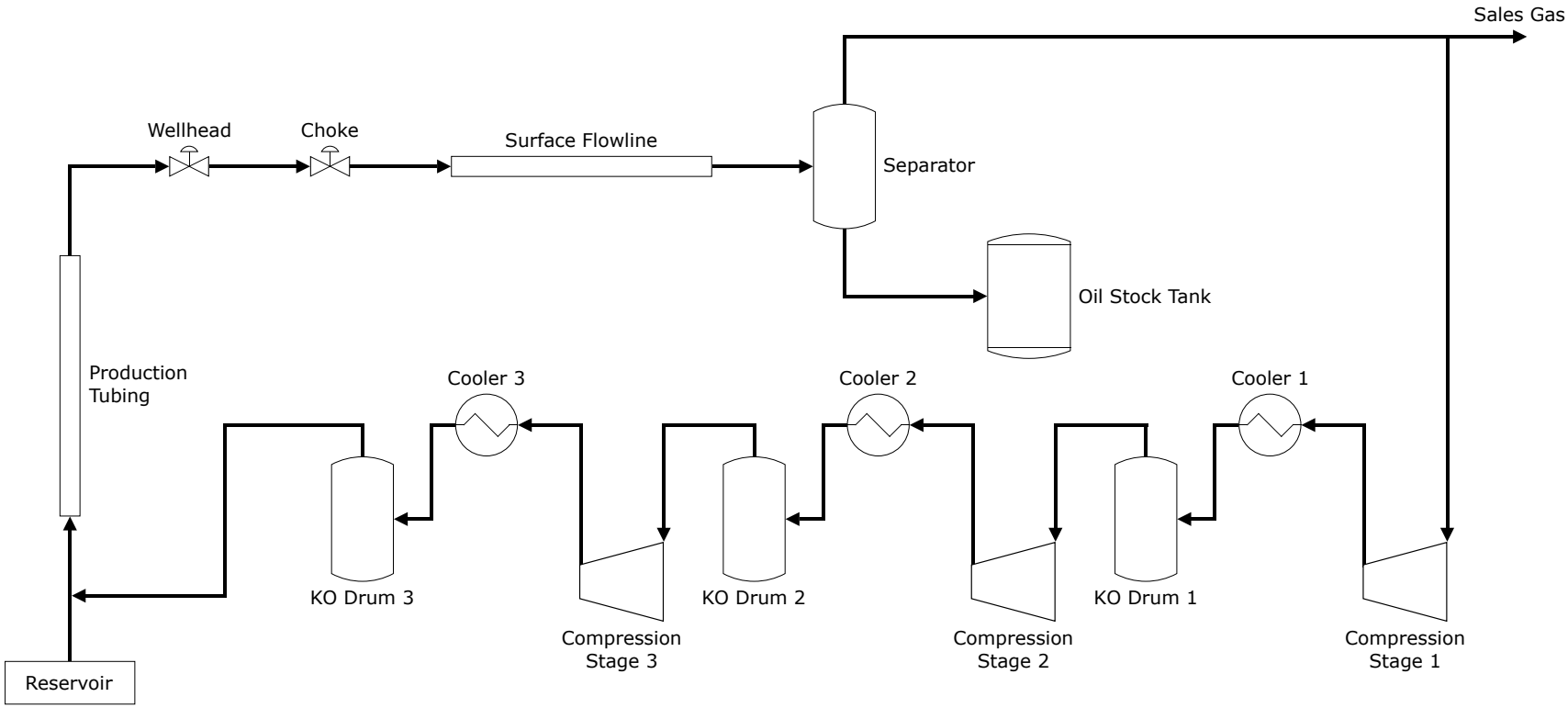

Figure 4.1: Gas-Lifted Well Process Flow Diagram

The behavior and production from wells is usually determined by conducting a stabilized well test. During the test, the bottomhole pressure, production rate, and gas oil ratio are measured. Oftentimes, additional tests are conducted at varying pressures to help generate a production curve and to examine how the characteristics of the well change with pressure. Well tests help production engineers to plan ahead as the well produces and manage the operation. For this base case simulation, it is assumed the well has been tested to have a production rate of 1200 bbl/d at a bottomhole pressure of 3200 psia. This single well test will be used to develop an IPR from the Darcy method and will be further discussed in Section 4.2.

Figure A.2 in the Appendix gives the flowsheet used in ProMax to model the process. The reservoir is not modeled directly, instead, the flow from the reservoir is given in the Well Fluid stream. The flow rate for this stream is determined by the simulation using the IPR implemented through custom calculators defined in the program. The well fluid next enters a pipeline block used to model the production tubing. The tubing is simulated as a 5000 ft long vertical pipe to account for the drop in pressure as the fluid rises to the surface. Flow through the production tubing will be multiphase because of the presence of both liquid and gas. To model the flow regime, the simulation uses a multiphase flow correlation of the user's choosing. In this case, the default correlation of Beggs and Brill was used and is based on Brill and Beggs (1991) and Brill and Mukherjee (1999). According to the ProMax Help files, the Beggs and Brill correlation can be used for any angle of inclination. The correlation first determines a flow pattern which would exist for horizontal flow and then determines the liquid holdup, or how much of the pipe contains liquid. There are several flow patterns which can be predicted by the correlation, and the patterns can be categorized as segregated, intermittent and distributed flow.

Additionally, the pipeline block in ProMax is capable of modeling the heat transfer to the environment as the fluid flows through the pipe. The software either uses a provided heat transfer coefficient of calculates one based on user input. The ambient temperature is modeled as a linear gradient from the reservoir temperature to the surface temperature. Properties specified in the pipeline block modeling the production tubing are given in Table 4.2 below.

Property	**Value**	**Units**
Total Length	5000	ft
Number of Segments	10	-
Outside Diameter	3	in
Absolute Roughness	0.0018	in
Multiphase Flow Correlation	Beggs and Brill	-
Ambient Temperature Gradient	24	°F/1000 ft
Material of Construction	Carbon Steel A106	-
Ground Type	Sandstone	-
Overall Heat Transfer Coefficient	2.745	BTU/(h*ft^2)

Table 4.2: Specifications used to Model the Production Tubing

After flowing up through the production tubing, the well fluid makes its way to the surface. The wellhead marks the end of the tubing and casing at the surface and serves as a pressure control device. The wellhead is modeled simply as a valve in the simulation and is used as a node in the IPR analysis. The choke is also modeled with a valve in the flowsheet, and the pressure at the wellhead is calculated with a user-defined empirical correlation for two-phase critical flow at a given flow rate. The relation, given in Equation 4.1, was first presented by Gilbert (1954), and several sets of values for the A coefficients have been proposed. Gilbert empirically found the values to be 3.86×10^{-3} for A_1, 0.546 for A_2, and 1.89 for A_3. The outlet pressure from the choke determines the production separator operating pressure. For both the base case and the recycle case, the choke is set to operate the production separator at 200 psig with an opening diameter of 30 in/64. The outlet pressure from the choke is slightly higher to account for the pressure drop in the flowline leading from the choke to the separator.

$$p_{wh} = \frac{A_1 q_L R^{A_2}}{d^{A_3}} \tag{4.1}$$

Where:

A_{1-3} = equation coefficients,

d = pipe diameter, in,

p_{wh} = wellhead pressure, psia,

q_L = liquid flow rate, bbl/d,

R = gas-liquid ratio, SCF/bbl

From the choke valve, the fluid flows through the surface flowline to the production separator. Oftentimes, a number of wells are linked together through flow lines to a common separator. The flowline is modeled as a 4 in nominal pipe which is 1000 ft in length and has a standard schedule. The heat transfer coefficient is again calculated by ProMax, similar to the production tubing. Provided heat transfer specifications include the same material of construction, a surface ambient temperature, and an above-ground pipe surrounding. The flow regime and resulting pressure drop are calculated using the Beggs and Brill multiphase flow correlation. Pressure drops in the flowline are much smaller than in the production tubing because it is a horizontal pipe, and there is no hydrostatic head to overcome.

The well fluid next enters the production separator. The simulation uses a two-phase separator block to model the production separator. This separator splits the inlet stream into gas and liquid streams with no entrainment. The software determines the phase concentrations based on the chosen thermodynamics package which would be Peng-Robinson in this case. The operating pressure can have a large impact on both the flow rate and composition of outlet streams because more gas is liberated as pressure is lowered. The separator operating pressure is set to 200 psig to ensure sufficient pressure to transport the sales gas in a pipeline.

In the base case, all gas from the production separator goes to a Sales Gas stream to be sold as product. None of this gas is used as lift gas, but for the optimized case, a portion of the gas will be compressed and re-injected into the well. The liquids from the production separator are sent to a heater treater unit. The heater treater is essentially a low pressure, three-phase separator which is used to break oil and gas or oil and water emulsions. Heat is applied to the oil to lower the viscosity and increase phase separation so the oil can meet pipeline specifications. The heater treater is modeled in ProMax as a three-phase separator block with an energy stream. An energy stream can be added to any separator in the software to include an additional degree of freedom in the unit operation. The heater treater is set to have an outlet temperature of 150 °F and an outlet pressure of 50 psig. The temperature of 150 °F should be sufficient to break any emulsions and liberate additional gas from the liquid phase. This liberation helps to reduce emissions from the oil stock tank where the oil will eventually end up. It is important to note the heater treater is modeled to have an outlet pressure of 50 psig and an inlet pressure of 200 psig from the production separator. In reality, this large pressure drop does not occur in the heater treater, but a valve upstream of the vessel. The valve could be modeled separately but doing so would not change the final state of the separated phases or the required duty to heat the fluid.

The oil phase exiting the heater treater is sent to the oil stock tank which holds the oil until it is ready for transport. The oil stock tank is modeled as a two-phase separator block because vapor emissions will separate from the oil at atmospheric pressure and over time. The outlet streams from the separator represent the gaseous emissions and the liquid sales oil. This separator also includes an energy stream which represents energy taken from the fluid by the environment as the oil cools to ambient temperature. An ambient temperature of 100 °F and a final pressure of 0 psig is set in the outlet streams to model the fluid from the oil stock tank. The gas phase exiting the heater treater is recombined with the gas from the production separator. To combine the two process streams, the gas from the heater treater must be compressed to 200 psig in the vapor recovery unit (VRU) compressor and cooled in the VRU cooler. An additional two-phase separator, the VRU knockout drum, is also used to remove any liquids which may have formed after compression and

cooling. The liquids collected from the VRU KO drum are returned to the heater treater with the liquid outlet from the production separator.

One additional simulation unit must be used in the model which is the recycle block. The recycle is necessary because the inlet to the heater treater includes a stream downstream of the block itself, as can be seen in Figure A.2. The program cannot solve the system sequentially and must instead iterate toward the solution. The mechanism for iteration is provided by the recycle block which adjusts the properties of the stream exiting the recycle block until they match the properties of the stream entering the block.

4.2 Inflow Performance Model

Fluids exiting the reservoir require energy to reach the surface. This energy is provided by the pressure of the fluid which is necessary to lift the fluids and overcome friction losses in the production system. The overall pressure drop of the fluid as it travels through the system is simply the pressure of the fluid at the reservoir, p_R, minus the pressure at the production separator, p_{sep}. The pressure drop through each component, whether it be the well face, the production tubing, the choke, or the surface flowline, depends on the flow rate through the component. In this way, pressure and flow rate are interconnected and cannot be solved separately. The pressure drop in a component may also vary with inlet pressure and, thus, the component pressure drops are also interconnected and cannot be solved independent of one another. The system must be solved as a whole and can be solved using a systems analysis approach known as NODAL™ Analysis[1].

NODAL™ Analysis was first applied to petroleum well production systems by Gilbert (1954) and involves dividing the system at a point or node. The system is then split into the inflow section upstream of the node and the outflow section which is all components downstream of the node. There must also be a relationship between flow rate and pressure drop for each component to evaluate performance for various flow rates. Additional constraints to solve the system include a single pressure at each node and equality between inflow and outflow at each node. Once these constraints are met, the flow rate through the system can be determined. Two pressures do not

[1]NODAL Analysis is a trademark of Flopetrol Johnson, a division of Schlumberger Technology Corporation.

vary at a particular time in the well's life which are the reservoir pressure and the production separator pressure. The pressure at a given node pressure can be calculated from the pressure drop downstream of the reservoir.

$$p_{node} = p_R - \Delta p_{inflow} \tag{4.2}$$

The pressure at the same given node can also be found using the pressure drop in the components downstream of the node and the separator pressure.

$$p_{node} = p_{sep} + \Delta p_{outflow} \tag{4.3}$$

The pressure drops in both the inflow and outflow components will vary with flow rate, therefore, a graph can be constructed plotting node pressure vs flow rate for both sides. The intersection of the two curves represents the same node pressure and the corresponding flow rate in the system. This graphical process is shown in Figure 4.2 below.

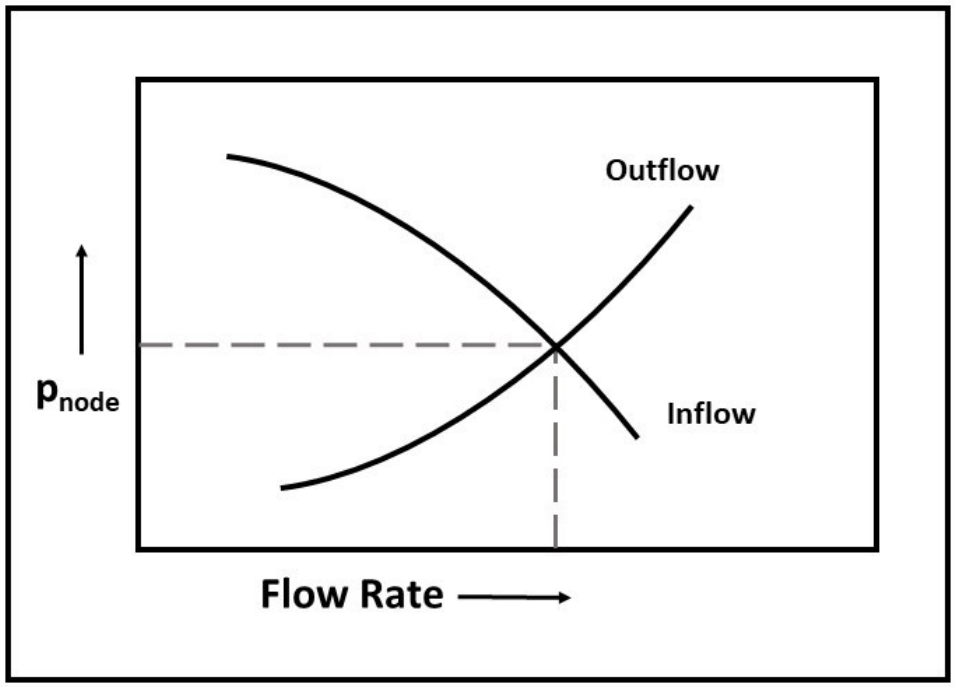

Figure 4.2: Node Pressure vs Flow Rate

The most frequently selected node solving this system is the bottomhole between the reservoir and the piping system. The purpose of dividing the system here is to separate it into a side for the reservoir behavior and a side for the piping system behavior. A pressure drop on the reservoir side is modeled using Darcy's equation. As previously discussed in the introduction and given in Equations 1.1 and 1.2, Darcy's equation estimates the pressure drop across a filter bed as a function of permeability, fluid velocity, and viscosity. This equation is incorporated into the IPR to provide a relation between reservoir production and pressure. When applied to reservoir production, Darcy's equation is typically simplified using a combined term known as the productivity index, J. The simplified form is given in Equation 1.3 and will be used to estimate the flow rate in this model for certain cases. The simplified form allows a single well test to estimate the productivity index. This is done by rearranging the simplified form to solve for J as given in Equation 4.4 below.

$$J = \frac{p_R - p_{wf}}{q_0} \tag{4.4}$$

It is important to note the productivity index depends on the pressure, and the estimates given by Equation 1.3 can be widely off if used at pressures largely different from the well test pressure. This will be the case when gas lift is used to decrease the bottomhole pressure, therefore, the model must be expanded to include this case. One particular pressure to note is the bubble point pressure of the reservoir fluid, p_b, because as the fluid drops below the bubble point gas is evolved. The evolved gas will change the flowing characteristics of the produced fluid and the Darcy model will no longer be accurate. The form of the equation used to determine the produced flow rate is determined by where gas evolves, and gas evolution will begin to occur when the pressure drops below the bubble point pressure.

If both the reservoir and bottomhole pressures are greater than the bubble point pressure, then Darcy's equation, Equation 1.3, is used. Darcy's equation corresponds to a constant productivity index, J. If both the reservoir and bottomhole pressures are less than the bubble point pressure, then Vogel's equation, Equation 1.4, is used to account for the change in the productivity index. If the reservoir pressure is greater than the bubble point pressure but the bottomhole pressure is

less than the bubble point pressure, gas will be evolved somewhere between the reservoir and the bottomhole. A hybrid between the Darcy and Vogel equations must be made to account for the change in productivity index when the pressure drops below the bubble point. The total production from the reservoir, q_0, has a Darcy contribution and a Vogel contribution. The Darcy contribution is calculated directly from Equation 1.3 and is labeled q_b below in Equation 4.5 because it corresponds to flow contributions above the bubble point.

$$q_b = J(p_R - p_b) \tag{4.5}$$

The Vogel contribution is found by replacing p_R in the Vogel Equation with p_b as the new upper pressure. Both q_0 and $q_{0(max)}$ must be discounted by q_b to account for the Darcy contribution. Equation 4.6 below gives this expression in the original form and Equation 4.7 gives a form solved for q_0 or the total flow including both contributions.

$$\frac{q_0 - q_b}{q_{0(max)} - q_b} = 1 - 0.2\left(\frac{p_{wf}}{p_b}\right) - 0.8\left(\frac{p_{wf}}{p_b}\right)^2 \tag{4.6}$$

$$q_0 = q_b + (q_{0(max)} - q_b)\left[1 - 0.2\left(\frac{p_{wf}}{p_b}\right) - 0.8\left(\frac{p_{wf}}{p_b}\right)^2\right] \tag{4.7}$$

The derivative of Equation 4.7 is found and evaluated at a value of p_{wf} greater than or equal to p_b to find an expression for J, because the productivity index is defined as the negative reciprocal slope. This evaluation produces Equation 4.8 which is solved for $(q_{0(max)} - q_b)$ and substituted into Equation 4.7 to give the final form for finding the produced flow rate, q_0, in Equation 4.9.

$$J = \frac{1.8(q_{0(max)} - q_b)}{p_b} \tag{4.8}$$

$$q_0 = q_b + \frac{Jp_b}{1.8}\left[1 - 0.2\left(\frac{p_{wf}}{p_b}\right) - 0.8\left(\frac{p_{wf}}{p_b}\right)^2\right] \tag{4.9}$$

4.3 Injected Gas Case

The injected gas simulation case begins with the same equipment as was used to model the base case. An inlet stream represents the production from the reservoir and a second stream is mixed with the inlet to model the injection gas at the bottom of the well. The injected gas will lower the density of the fluid column rising up the tubing, allowing for a lower bottomhole pressure. A lower bottomhole pressure will affect the IPR from the reservoir and can increase production which is the aim of using gas lift.

Mixed well fluid and injected gas passes through the pipeline block which models the production tubing. The same properties will be used to model the production tubing for the injected gas case as was used in the base case, and these properties can be found in Table 4.2 above. The fluid then reaches the surface and again passes through the wellhead and choke valves. These valves will be modeled in a similar manner as before, with Gilbert's two-phase critical flow relationship again being used to estimate the pressure drop in the choke. The surface flowline and production separator are also simulated in the same manner as before. However, the gas coming off the top of the production separator will be split into a sales gas stream as product and a recycled stream to be used as the injection gas. The liquids stream from the production separator follows an identical path as the base case, including the heater treater, VRU compressor, and oil stock tank.

It is important to remember the system is modeled as a steady-state process so a fixed ratio of gas must be selected to split from the sales gas for reinjection. The split ratio is the key parameter for optimizing the system, as too much gas can cause the pressure losses in the production tubing to dominate the system, and too little gas will not produce additional fluids from the reservoir. ProMax provides the user the capability to define a solver or a property for optimization. From the ProMax help files, the solver is used to "[A]chieve a given condition which cannot be set directly." The solver will iteratively change a particular stream or block property to maximize an objective function defined by the user. In this case, a solver can be used on the split ratio to maximize the flow rate of oil produced from the stock tank. Alternatively, the simulation can be solved a number of times for different values of the split ratio and a resulting curve can be plotted to determine the

optimal value.

After being split from the sales gas, the injection gas is compressed again so that it can be sent to the bottom of the well. Wells may have different points of injection depending on the pressure of the lift gas available and the needs of the well. There is a tradeoff when deciding where to inject lift gas. If gas is injected lower in the well, a higher injection pressure is required, but the gas helps to lift a larger portion of the well fluid in the tubing, whereas, with a higher injection point a lower injection pressure is required but less of the fluid column is affected by the lift gas. Production is maximized by lifting the well fluid from immediately above the producing zone which will be the case in this model. Compression occurs in three stages with the following pieces of equipment in each stage.

i. Compressor Stage

ii. Air Cooler

iii. Knockout Drum

Each compression stage is modeled with a compressor block in the simulation. The initial pressure is set by the operating pressure of the production separator, and the final compression pressure is set by the well fluid pressure. The gas is compressed to a pressure such that, after traveling through the production casing, the well fluid pressure and injection gas pressures are the same. Referring to Figure A.3, a solver is set in stream 20 with an objective function minimizing the difference between pressures at the bottom of the well. Each compressor block is specified with a polytropic efficiency of 70% and a compression ratio. The compression ratios are set equal to one another to minimize compression power and to balance the compression load between the three stages. If there was no pressure drop between stages, the stage compression ratio would simply be the cube root of the overall compression ratio. However, the interstage cooling pressure drops must be accounted for when setting these compression ratios. Only two degrees of freedom remain to specify pressure, because the inlet and outlet pressures are already set. The second stage compression ratio is set to equal the first, and a solver is used to set the first and third stage

compression ratios equal to each other. This setup ensures the compression ratios remain equal, regardless of how the pressure may change in the production separator or well fluid.

As the gas is compressed, it heats up significantly so interstage cooling is required to cool the gas again. A single-sided heat exchanger simulates the cooler, and the specifications include a pressure drop of 5 psi and a conservative 120 °F outlet temperature. After cooling and compression in each stage if any liquids have formed, they are removed in the knockout drums which are modeled as two-phase separators in the simulation. The only specification required for a separator with no energy stream is a pressure drop which is specified to be 0 psi. Another recycle block is required to re-inject the gas into the well, because the lift gas comes from the well fluid and iteration is required to approach the system solution.

To solve this system using the previously discussed IPR, an iterative process is required. Figure 4.3 below is a flowchart, which outlines the steps performed by the simulation to reach a system solution. This iterative process is also performed for the base case, as the same relationship between flow and pressure exists in the reservoir and piping sections. Additional loops are required for the two recycle blocks and the solver on the casing inlet pressure, but the flowchart illustrates the process of determining the reservoir pressure and production rate simultaneously.

First, a value for the bottomhole pressure, p_{wf}, is selected to begin the iterations. The production rate, q_0, corresponding to this flowing bottomhole pressure is calculated from the IPR. The IPR calculation is broken up into three possible regions based on whether gas is evolved in the reservoir, the bottomhole, or between the two. Next, the pressure drop in the production tubing is calculated via simulation with the given input from the bottomhole pressure and production rate. The wellhead pressure is then calculated using Gilbert's two-phase critical flow equation and the flow rate calculated earlier. The node selected for this NODAL™ Analysis is the wellhead block which acts as a dummy valve in the model. The stopping criterion for the iterations is a wellhead pressure drop of 0 psi which indicates the inflow and outflow balance one another. If the wellhead pressure is not zero, the simulation software uses an optimization algorithm to step towards the solution until the pressure drop in the wellhead is sufficiently close to 0 psi. In the base case,

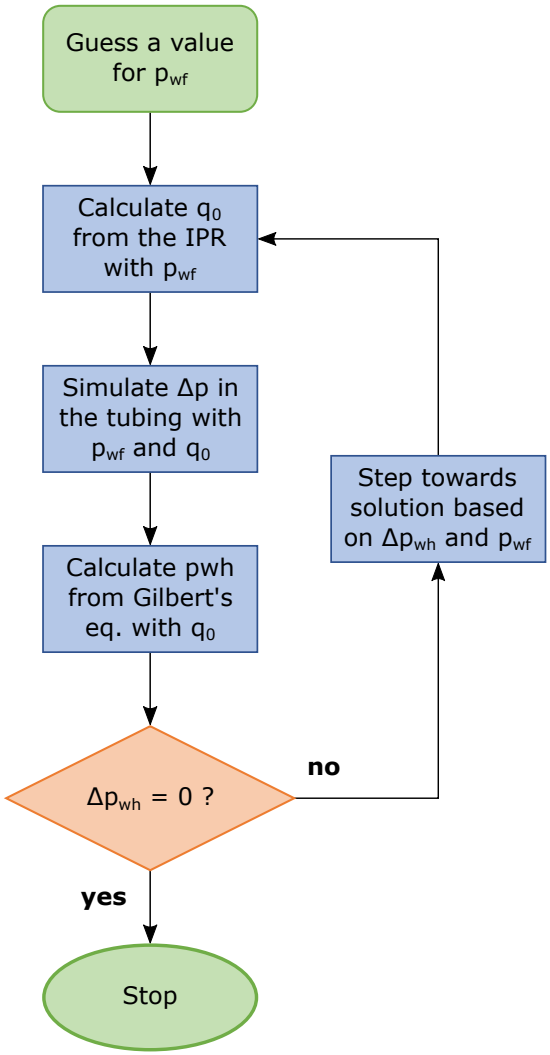

Figure 4.3: IPR Iterative Solution Flowchart

which does not have gas lift, this process of iteration only occurs once, and the rest of the process can be solved. However, in the gas lift case, the lift gas is a recycled stream. To solve the system for the recycled lift gas and reservoir properties two different iteration loops must be solved with the lift gas loop being outside of the reservoir loop. The order in which iterative loops are solved can be specified by the user in the program using priority values. A higher priority corresponds to an inner loop, and, in this case, the IPR solver is the inner loop and gets a higher priority value.

4.4 Economic and Sustainability Analysis

An incremental and high-level economic analysis will be performed to determine if the potential gain in revenue is worth the cost of compression needed to implement gas lift. The results of the base case will be compared with the optimized gas lift case to evaluate the incremental production increase. When examining potential projects which are incremental in nature, a company should choose those projects that are economically viable, independent of the economics of the larger project. The threshold which determines economic viability is set by the company considering the project.

Both the fixed and operating costs associated with gas lift will be considered along with the potential metrics the company may want to include to ensure a sustainable process. The source of revenue for the gas lift process will be the incremental increase in oil and gas production resulting from its implementation. Prices used for these expenses and products are given in Table 4.3 below. The prices of crude oil and natural gas are based on the average price from 2018 - 2019, and other values, such as the discount and inflation rate, are based on commonly used values (Mahmudi and Sadeghi, 2013).

Parameter	**Value**	**Units**
Price of Oil	61.11	$/bbl
Crude Treatment	2.00	$/bbl
Price of Gas	2.86	$/MSCF
Injection Cost	2.50	$/MSCF
Discount Rate	10	%
Inflation Rate	2	%

Table 4.3: Parameters Used for Economic Analysis

After conducting a traditional incremental return on investment analysis, another incremental return on investment analysis will be done with the addition of sustainability parameters, as discussed in the introduction. Several factors affecting sustainability exist in the project, including CO_2 emissions from power generation for the compressors and heat exchangers and stock tank flash emissions. These factors will be integrated into the incremental ROI calculation by using the SWROIM parameter developed by El-Halwagi (2017), given in Equation 1.11.

The additional capital investment required to implement gas lift consists of a three-stage compressor with interstage cooling provided by heat exchangers and separators to remove any liquid from the compressed gas. Estimates for the capital costs associated with these pieces of equipment can be made using cost curves provided by Towler and Sinnott (2013). The form of the cost curve is given by Equation 4.10 with estimated costs given on a January 2010 basis. The Chemical Engineering Plant Cost Index (CEPCI) for this month was 532.9 and will be used to adjust costs to a January 2019 basis, as this basis was the most recent available. This basis also fits well with the material estimates given previously as an average over the years 2018-2019.

$$C_e = a + bS^n \tag{4.10}$$

Where:

a, b = correlation coefficients,

C_e = purchased equipment cost on a January 2010 basis,

n = equipment exponent,

S = equipment size parameter

Values for the correlation coefficients, equipment exponents, and size parameter bounds are given by Towler and Sinnott (2013) for various types of equipment are given in Table 4.4 below. Towler notes the correlations are only valid if the size parameter, S, is between the provided bounds given in the table, and, unless otherwise noted, the equipment is made of carbon steel. If necessary,

the price for equipment made of other materials can be estimated by extrapolating the calculated value of C_e using material factors.

Equipment	**Units of** S	S_{lower}	S_{upper}	a	b	n
Compressor	power, kW	93	16,800	260,000	2,700	0.75
Heat Exchanger	area, m^2	1.0	500	1600	210	0.95
Pressure Vessel	mass, kg	160	250,000	11,600	34	0.85

Table 4.4: Cost Curve Parameters

The cost estimates calculated by the correlation given in Equation 4.10 must be updated to prices in 2019. Updating costs is done by using the basis cost index, which is 532.9 for the month of January 2010 according to CEPCI. The cost index for the desired month, January 2019, is also needed which is 618.7 according to CEPCI (2020). Based on these two cost indices, the estimated purchase cost of equipment is updated according to the following equation.

$$Cost\ in\ year\ A\ =\ Cost\ in\ Year\ B\ \times\ \frac{Cost\ index\ in\ year\ A}{Cost\ index\ in\ year\ B} \tag{4.11}$$

Final equipment costs will also include additional costs for installation, engineering and procurement, delivery, and contingency. These costs can be approximated as a percentage of the purchase cost calculated using Equation 4.10. The purchased equipment costs cannot be calculated until the size of the equipment is determined from simulation results. Alternatively, the capital investment can be calculated from a reference plant of a similar process. The cost from the reference plant can be updated according to the flow rate through the equipment using the six-tenths rule given below in Equation 4.12. The exponent in the equation accounts for economics of scale which make larger operations more cost effective.

$$C_B = C_A \left(\frac{S_B}{S_A} \right)^{0.6} \tag{4.12}$$

C_A and C_B are the two plant capital costs and S_A and S_B are the flow rates of the two plants as a measurement of scale. Similar to the cost curve estimation, the capital costs must also be updated to current dollars using a CEPCI value. The incremental ROI calculated by the economic analysis will provide a basis for comparison with an incremental sustainability return on investment. The ISWROIM will incorporate metrics of sustainability with economic indicators for assessing the project.

The sustainability metrics chosen for the analysis are the carbon footprint and total annual stock tank emissions. Target values for CO_2 and stock tank emissions will be based on the base case values found after simulation. A decrease in the amount of CO_2 or stock tank emissions as compared to the base case will contribute positively towards the ISWROIM while an increase in emissions will take away from the metric. The weighting of these terms, w_i, will depend on their relative importance compared to net profit to the decision makers. For the purpose of this model, both parameters will be given a weighting of 0.1 or 10% of the importance of net profit.

The carbon footprint of the process is evaluated by following the EPA's method for stationary combustion sources (EPA, 2016). This method assumes all heating utilities are fueled by natural gas with a carbon content of 14.47 kg C/MMBTU, a heat content of 1029 BTU/SCF, and complete oxidation. Electric power generation, used for the heat exchangers and compression in the incremental project, has an emission factor of 0.73 tonne CO_2/MWh. The calculation of stock tank emissions will assume all gases flashed at stock tank conditions are emitted to the atmosphere.

5. RESULTS AND DISCUSSION

The results from the presented methodology are given below for the base case without recycle, the inflow performance relationship, the gas lift case with recycle, and the economic and sustainability analysis. The two operating cases will be compared to give an understanding of how gas lift affects the process with the assumed conditions. The economic and sustainability analysis will attempt to quantify whether this gas lift should be implemented for the given well to improve the overall production process.

5.1 Base Case

The simulation flowsheet for the base case created in ProMax is given in the Appendix as Figure A.2. The software uses a sequential solver algorithm to individually calculate operating conditions of each stream and block starting from the inlet. In addition, several user-defined calculators are included for the implementation of the IPR calculations which determine the production rate from the reservoir, the bottomhole pressure, and the wellhead pressure upstream of the choke valve. The flowsheet will continue iterating until all solvers on the flowsheet have minimized their respective objective functions below a given threshold.

The base case and the case with recycle will be modeled with the same reservoir conditions, which are an average pressure of 3800 psig and a temperature of 200 °F. After solving for the reservoir production and bottomhole pressure according to the IPR relationship and following the procedure given in Figure 4.3, the reservoir fluid is predicted to have the properties given in Table 5.1. The temperature at the bottomhole is assumed to be the same as the reservoir temperature of 200 °F. The software predicts a bubble point pressure of 3020 psia for the fluid with the given composition and temperature. This pressure is between the final bottomhole pressure of 2125 psia and the reservoir pressure of 3800 psig, which implies gas is liberated somewhere between the reservoir and the opening to the well. The hybrid Darcy and Vogel relationship given in Equation 4.9 must be used to find the predicted flow rate. The mole fraction vapor is found by the simulation

using a flash calculation at the given temperature, pressure, and composition. The molecular weight is calculated by the software using the composition of the stream and the predicted oil properties.

Property	**Value**	**Units**
Temperature	200.0	°F
Pressure	2125	psia
Bubble Point Pressure	3020	psia
Mole Fraction Vapor	17.30	%
Std Liquid Volumetric Flow Rate	2374	bbl/d
Molecular Weight	107.5	lb/lbmol

Table 5.1: Base Case Bottomhole Fluid Properties

As the fluid moves to the surface through the production tubing, the pressure drops due to frictional forces and hydrostatic head. The pipeline block in the simulation calculates a pressure drop of 1232 psi using the Beggs and Brill multiphase flow correlation. The heat transfer calculations in the pipeline predict a drop in temperature, as the surface is cooler than the reservoir temperature, and the outlet temperature is simulated to be 157 °F. These changes to the pressure and temperature result in a net liberation of gas, and as the fluid exits the tubing, the mole fraction vapor has increased from 17.3 to 35.4%.

The Gilbert choke equation estimates a wellhead pressure of 893 psia for the given flow rate which closely matches the outlet pressure from the production tubing and represents the stopping criterion for the inflow and outflow balance. The choke outlet pressure is 223 psia which sets the production separator operating pressure at 200 psig after the pressure drops in the surface flowline. Neither the pressure nor the temperature change much in the flowline because it is relatively short

with no change in elevation.

With the dramatic change in pressure from the wellhead to the production separator, the fluid has dropped in temperature from 157 to 134 °F, and additional gas has been liberated to again increase the mole fraction vapor from 35.4 to 49.4%. The separator splits the gas towards the sales gas stream and the liquid fraction exits the bottom of the separator to the heater treater. The 50.6% mole fraction of liquid equates to a standard liquid volumetric flow rate of 1873 bbl/d. This liquid stream combines with the recycled stream from the knockout drum and enters the heater treater which heats the liquid to 150 °F and drops the pressure to just 50 psig. The increase in temperature and decrease in pressure results in a standard volumetric vapor flow rate of 84.7 MSCFD of gas off the top.

The gas is compressed in the VRU compressor to 200 psig and the temperature is reduced to 120 °F in the VRU air cooler. A small amount of liquid drops out of the gas after compression and cooling; this gas is removed in the VRU knockout drum and recycled to the heater treater inlet. The compressed gas is combined with the gas stream from the top of the production separator to make the sales gas stream. The liquids from the heater treater move to the oil stock tank which sits at ambient conditions of 100 °F and 0 psig. The final oil production rate from this operating point is 1799 bbl/d with an emissions rate from the stock tank of 41.8 MSCFD. The sales gas is delivered from the process at 132 °F and 200 psig at a standard vapor volumetric flow rate of 1163 MSCFD. The composition for both the sales oil and sales gas streams are given below in Table 5.2.

The solved flowsheet indicates the heater treater set points of 200 psig and 150 °F will require a heat duty of 210 MBTU/h. This heating utility is assumed to be supplied by stationary combustion sources as part of the carbon footprint evaluation of this process in the Economic and Sustainability Analysis. The simulated VRU compressor requires 8.36 hp assuming a 70% polytropic efficiency. The EPA's estimation for emissions due to electrical power generation will be used to account for emissions from the compressor. The VRU cooler is assumed to be a fin fan exchanger and the removed heat from the gas stream is calculated to be 27.9 MBTU/h. The cooling utility will contribute to the CO_2 emissions calculation by approximating the power required to run the fin fan

heat exchangers.

Component	**Sales Gas**	**Sales Oil**
N_2	1.13	4.83×10^{-5}
CO_2	0.256	1.35×10^{-3}
C_1	73.0	0.0711
C_2	12.2	0.496
C_3	7.94	2.61
iC_4	1.12	1.17
nC_4	2.58	4.11
iC_5	0.622	2.37
nC_5	0.681	3.38
C_6	0.453	6.10
C_{7+}	1.28×10^{-4}	79.7

Table 5.2: Compositions of Sales Streams from Base Case in Mole %

The table above shows the compositions of the two product streams which are split from the reservoir fluid composition. The largest determining factor for these compositions is the operating conditions of the production separator. Although the majority of gas leaves the oil for the sales gas stream, a fraction of the oil contains methane, ethane, and propane which make up the bulk of emissions from the oil stock tank. A table of stream properties for all streams in the base case simulation is given in the Appendix in Table A.1. The streams are numbered similarly to the recycle case process streams which allows a direct comparison of streams from one case to the

other. Values in Table A.1 which contain an asterisk indicate the stream property is specified either directly by the user or by a calculator created by the user.

5.2 Inflow Performance Model

The equations describing the inflow performance model discussed previously were used to predict the production rate from the reservoir from a given well flowing pressure, p_{wf}. From the assumed single well test data, the productivity index, J, is calculated using Equation 4.4 with a resulting value of 1.51 bbl/psi. The productivity index is used in both the Darcy and Vogel equations for estimating the production rate from the reservoir as a function of the bottomhole pressure. These relations are used together depending on where vapors form to account for the changing flow characteristics of the well fluid as gas evolves. Figure 5.1 below shows the IPR used to model the reservoir for this process.

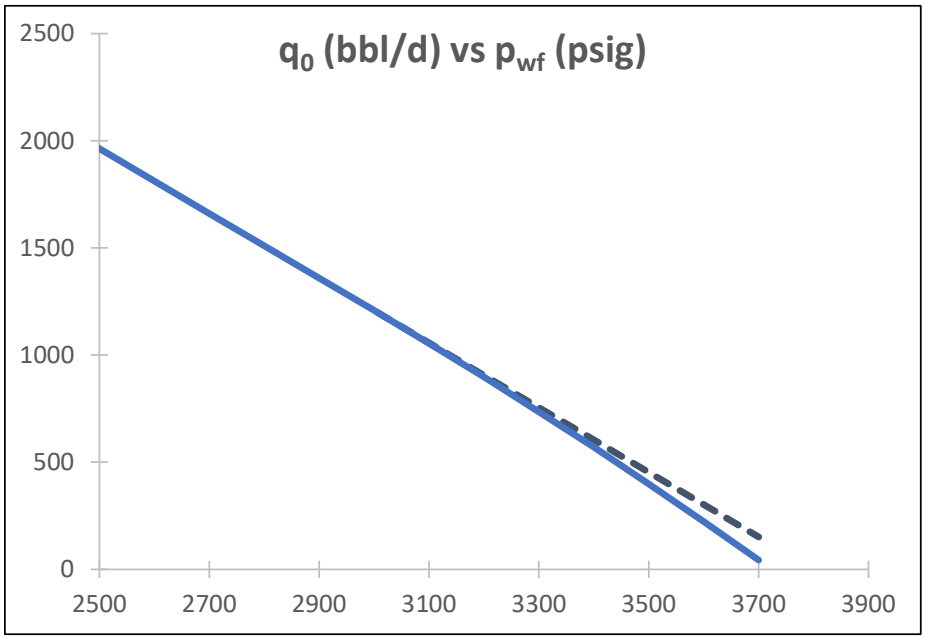

Figure 5.1: IPR Plot Modeling Reservoir Behavior

The solid line is the IPR curve which includes the Darcy equation, Equation 1.3, and the Darcy-Vogel hybrid equation, Equation 4.9. The Vogel equation, Equation 1.4, is not used because the reservoir pressure, p_R, is always assumed to be above the bubble point pressure, p_b. The dashed line is only the Darcy equation and demonstrates the modification the Darcy-Vogel hybrid makes to the IPR. The difference is small in this case because the maximum well flowing pressure is equal to the reservoir pressure which is not much greater than the bubble point pressure. This means the ratio $\frac{p_{wf}}{p_b}$ will never be much more than one, and the hybrid equation is similar to the Darcy equation. The maximum value the ratio of pressures can take occurs when the $p_w f$ is equal to the reservoir pressure and production ceases. If the reservoir pressure is much greater than the bubble point pressure, a greater deviation from the Darcy equation would occur to account for the difference in flowing characteristics.

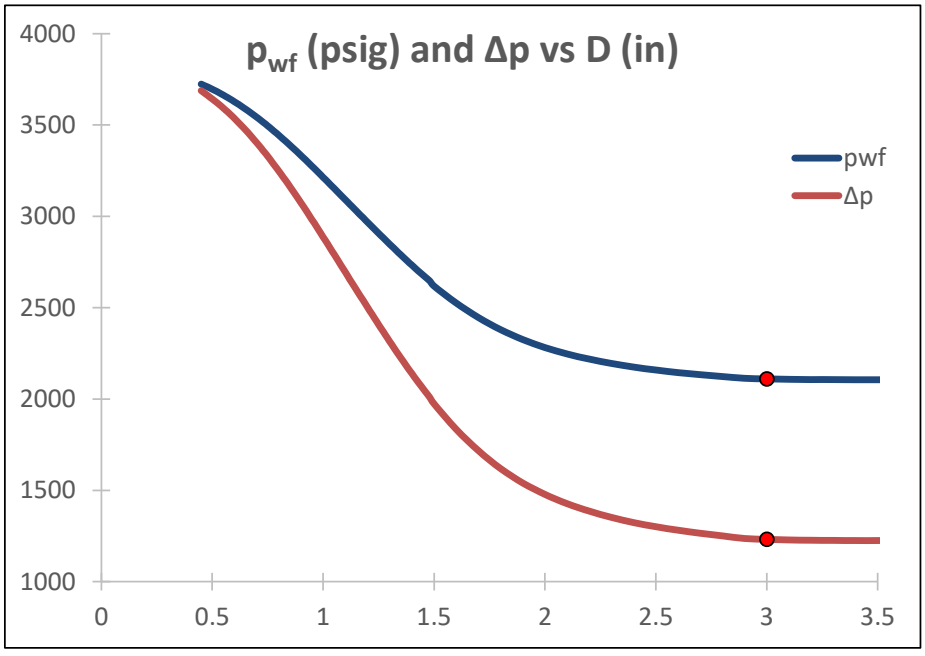

Figure 5.2: Base Case Well Fluid Pressure and Tubing Pressure Drop with Tubing Diameter

Figure 5.2 above shows the relationship between the well fluid pressure and tubing pressure drop vs the tubing diameter, D. At larger values of D, the pressure losses are smaller because frictional losses are not substantial. For a smaller pressure loss in the tubing, the well fluid pressure can be lower and increase production. The red dot in Figure 5.2 gives the operating point for the base case with a well fluid pressure of 2110 psig which corresponds to a pressure loss of 1232 psi in the tubing at a diameter of 3 in. As the tubing diameter decreases, frictional losses in the tubing have a greater impact, increasing the tubing pressure loss. The increase in tubing pressure loss must be overcome by an increase in the well fluid pressure to drive the oil and gas to the surface.

The impact of tubing size on the production rate, q_0, is given below in Figure 5.3. Again, the red dot indicates the operating point for the base case simulation with a production rate of 2374 bbl/d for a tubing diameter of 3 in. The simulation was solved for a number of possible tubing diameters from 0.5 to 3.5 in to produce the plots in Figures 5.2 and 5.3. The inverse relationship between well fluid pressure and production rate can be seen by comparing these plots.

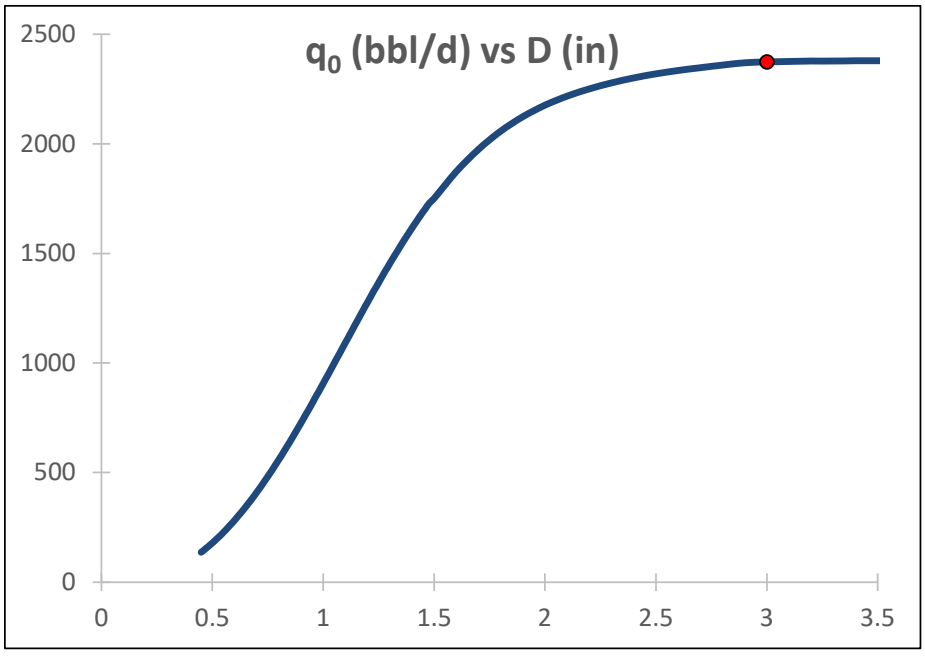

Figure 5.3: Effect of Varying Tubing Diameter on Production Rate

The relationship between production rate and tubing diameter indicates the base process will not be improved by increasing the tubing size. The increase in tubing size would come with diminishing returns as the curve flattens out. However, this may not be a good idea because the increase in tubing size could decrease the velocity of the fluid until the liquids cannot be lifted to the surface. This problem becomes more likely to occur over the life of the well, as production inevitably decreases.

Another characteristic of note in Figure 5.2 is the similarity between the well fluid pressure curve and the tubing pressure drop curve. The tubing pressure losses increase faster with decreasing tubing size until the two are equal. When the curves intersect, a situation arises in which the well fluid requires all its pressure to reach the surface, and, beyond this point, well fluid will not reach the surface. The point these curves cross is predicted to be about 0.5 in for the tubing diameter. The well fluid pressure curve also approaches the reservoir pressure of 3800 psig asymptotically with decreasing tubing diameter because the well fluid pressure can never exceed the reservoir pressure. The difference between the well fluid pressure curve and the tubing pressure drop curve also represents the maximum operating pressure of the production separator for the given tubing diameter. For this reason, the process with the current reservoir conditions has a minimum tubing diameter of about 0.8 in before the production separator pressure drops below 200 psig.

A similar analysis was carried out to determine the response of the system to changes in the choke diameter setting. The diameter of the choke opening, measured in 64ths of an inch, was varied from 2 to 100 in/64. The system was solved for each choke diameter using the iterative IPR method given in Figure 4.3, and for each setting, the resulting well fluid pressure, production rate, and wellhead pressure were all recorded. The results of this analysis are given in Figure 5.4 below. The red dots in Figure 5.4 give the choke diameter for the base case simulation results, wherein, the choke diameter is set to 30 in/64. This choke setting corresponds to a well fluid pressure of 2110 psig and a wellhead pressure of 879 psig.

The difference between the well fluid pressure curve in blue and the wellhead pressure curve

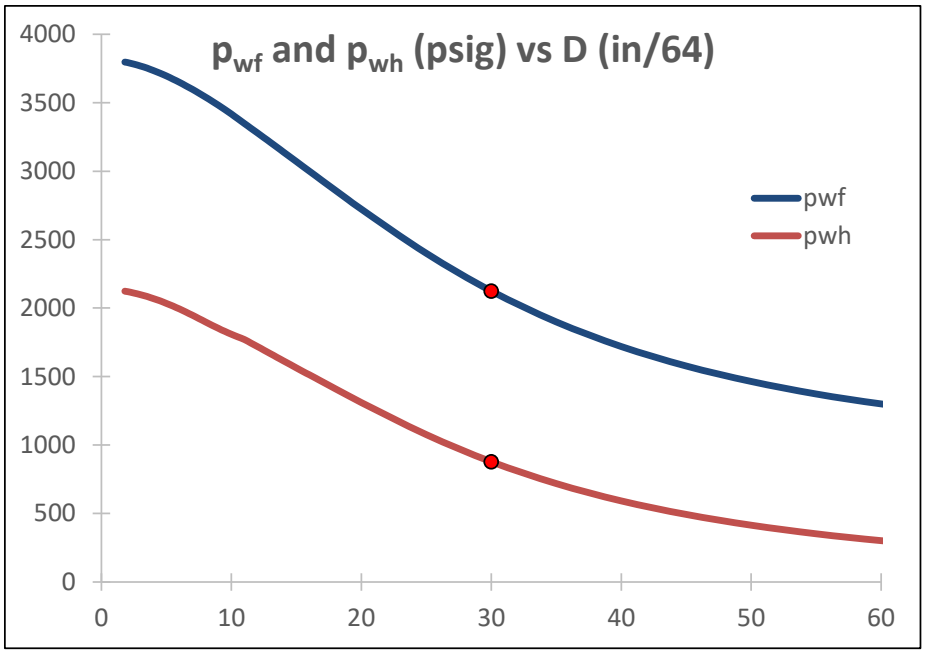

Figure 5.4: Well Fluid and Wellhead Pressures with Varying Choke Diameter

in red represents the pressure drop in the production tubing between these two pressures. The production rate curve resulting from this well fluid pressure curve would take a similar form to the graph in Figure 5.3 with production rate increasing as the well fluid pressure decreases and leveling off in a similar fashion for larger choke openings. The plot of pressure vs choke diameter demonstrates the impact the choke can have on the process. If the choke is set to a small value, the production rate can rapidly decrease as the choke begins to limit the process.

The graph above is only given up to a choke diameter of 60 in/64 because, above this value, the wellhead pressure drops below 200 psig which would impact the operation of the production separator. Similar to the analysis carried out on the size of the production tubing, the well fluid pressure curve in Figure 5.4 asymptotically approaches the reservoir pressure of 3800 psig as the choke diameter is reduced to zero. This occurs because the pressure required for the fluid to pass through the choke grows as the opening shrinks, but the available pressure is limited by the reservoir pressure.

5.3 Injected Gas Case

As discussed in the methodology, the injected gas case is similar to the base case with the addition of a compression station and associated equipment. A portion of the sales gas stream is split from the outlet of the production separator, compressed, and re-injected through the casing to help lift additional liquids to the surface. From a simulation standpoint, the injected gas will decrease the density of the liquids and reduce the pressure drop as the well fluid moves to the surface. This results in a decrease in the well fluid pressure and a corresponding increase in the production rate from the reservoir.

The new operating variable introduced in the recycle case is the fraction of gas split from the production separator for re-injection. A range of split fractions from 0 to 97.5% were set in the simulation and the system solved for each one. The resulting flow rates of liquids from the oil stock tank is given in Figure 5.5 as a function of the split fraction.

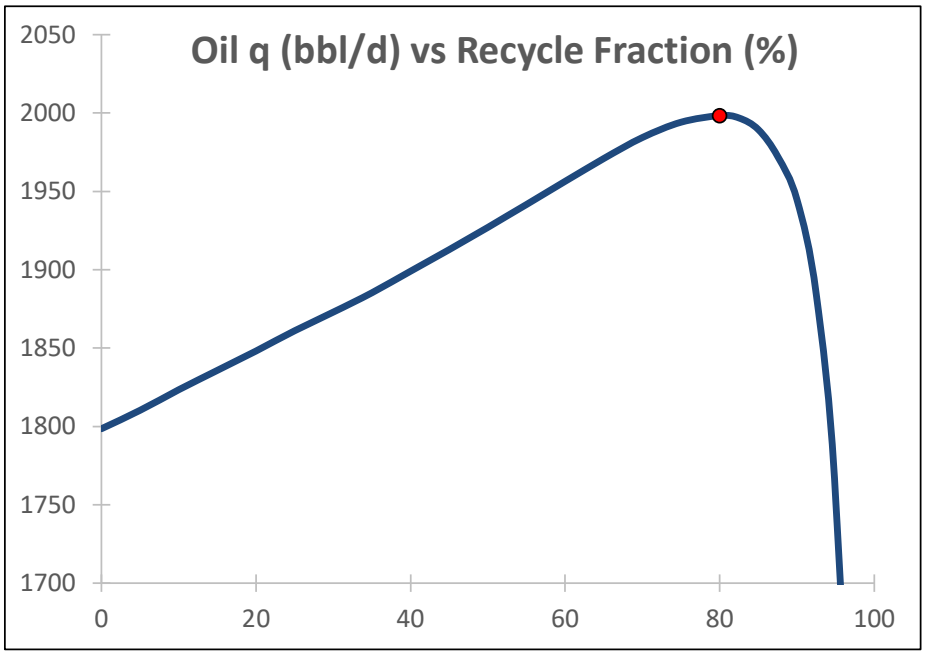

Figure 5.5: Oil Stock Tank Production as a Function of Recycled Gas Fraction

The split fraction of 0% corresponds to the base case and has the same flow rate of 1799 bbl/d from the stock tank. The curve above demonstrates the effect lift gas has on the system, with an increase in production at lower recycle fractions. Eventually, as the fraction of recycle gas increases and more gas mixes with the produced fluids in the bottomhole, the larger fraction of gas moving through the production tubing increases the pressure drop. The increased pressure drop negates the reduced density of the fluid, and production decreases. This relationship is reflected in the graph which first shows increased production with increasing split fraction before the production peaks and subsequently falls with greater fractions of lift gas. From Figure 5.5 above, the optimal value for the split fraction is 80%. The properties of the fluid produced by the reservoir and the combined stream, which includes the lift gas, are given in Table 5.3 for this optimal case.

Property	**Units**	**Reservoir Fluid**	**Combined Fluid**
Temperature	°F	200.0	179.5
Pressure	psia	1883	1883
Bubble Point Pressure	psia	3020	6350
Mole Fraction Vapor	%	21.60	70.17
Molar Flow Rate	lbmol/h	265.6	774.8
Molecular Weight	lb/lbmol	107.5	50.95

Table 5.3: Reservoir and Combined Fluid Properties

The combined well fluid and lift gas next enter the production tubing which is simulated to have a pressure drop of 1383 psi. This is a reduction of 80 psi from the base case which had a pressure drop of 894 psi. This reduced pressure drop in the tubing helps to lower the bottomhole pressure by 242 psi, as compared to the base case, and increases the reservoir production from 2374 to 2629

bbl/d. Another result of a lower bottomhole pressure is an increase in the mole fraction vapor of the produced fluids from the reservoir from 17.3 to 21.6%. As the combined reservoir fluid and lift gas rise to the surface, the pressure drops, gas is liberated, and the temperature decreases. The outlet temperature from the tubing is estimated to be 144 °F, and the mole fraction vapor increases from 70.2 to 74.8%.

The pressure has also dropped to match the predicted wellhead pressure from the Gilbert choke equation of 989 psia. The fluid passes through the choke and drops to a pressure of 268 psia. This pressure downstream of the choke is higher than the base case pressure of 223 psia, as the flowline pressure drop is predicted to increase from 8.35 to 53.7 psi with the increase in flow rate. The fluid arriving at the production separator has a pressure of 200 psig, and its mole fraction vapor has further increased to 82.2%. The decrease in pressure over the choke valve and flowline has further cooled the fluid from 144 to 113 °F.

The production separator splits the combined well fluid into a gas stream with a flow rate of 5797 MSCFD and a liquid stream with a flow rate of 2097 bbl/d. Both of these flow rates have increased from the base case separated streams, which had gas and liquid flow rates of 1078 MSFCD and 1873 bbl/d, respectively. Similar to the base case, the liquid stream from the separator is combined with a recycle stream and moves to the heater treater where the temperature and pressure are set to 150 °F and 50 psig. The increase in temperature and decrease in pressure liberate 116 MSCFD of gas off the top of the unit. The gas is compressed back to 200 psig to be combined with the sales gas stream. The VRU compressor, cooler, and knockout drum set the gas pressure and temperature to 200 psig and 120 °F. The small flow rate of liquid from the knockout drum returns to the heater treater as a recycle.

From the heater treater, the process liquid enters the oil stock tank, and its properties drop to ambient conditions of 100 °F and 0 psig. The oil stock tank model predicts a final sales oil flow rate of 1998 bbl/d which is an increase of 200 bbl/d from the base case. The emissions from the top of the stock tank are simulated to have a flow rate of 50.9 MSCFD, increasing 9.13 MSCFD from the base case.

The gas from the top of the separator is split into sales and injection gas streams, according to the injection gas split fraction, which has been optimized to maximize production. The injection gas has a flow rate of 4638 MSCFD, while the final sales gas stream combined with the VRU stream has a flow rate of 1275 MSCFD. The final sales gas flow rate is an increase of 112 MSCFD, as compared to the base case.

The injected gas moves to the three-stage compression station where it is compressed, cooled, and separated from any produced liquids three times in series. The final pressure is set, such that, when the injected gas meets the reservoir fluid, they have the same pressure. This specification is set using a solver on the pressure upstream of the casing until the condition is satisfied. Each cooler is set to have an outlet temperature of 120 °F with a 5 psi pressure drop. The compression ratio of all three compressors are set equal to one another using one specifier and one solver. Two calculators are used instead of three here, because only two degrees of freedom remain after the initial and final pressures for the compression train have been set.

The simulation solves this system to predict a casing inlet pressure of 2218 psia and a compression ratio of 2.19 in each compressor. As the gas moves through the casing, the pressure drop is predicted to be 334 psi, resulting in an outlet pressure of 1883 psia to match the well flowing pressure in the bottomhole. The compositions for the sales gas and sales oil streams are given in Table 5.4 below. The compositions of the product streams from the base case and the injected gas case can be compared using Tables 5.2 and 5.4. This comparison finds the product streams for both cases have nearly identical compositions, meaning the addition of lift gas does not significantly affect product stream composition for this process.

The changes in heating and cooling utilities, in addition to increased stock tank emissions, will be used to determine the sustainability of the lift gas process. The heat duty required by the heater treater has increased in the injected gas case from 210 to 496 MBTU/h with the increased production. The compressor power required by the VRU is now predicted to be 11.4 hp, and the VRU cooler now removes 38.6 MBTU/h from the gas stream off the heater treater. Additional power is also required to operate the compression train and associate coolers. The total cooling

Component	Sales Gas	Sales Oil
N_2	1.13	3.96×10^{-5}
CO_2	0.259	1.24×10^{-3}
C_1	73.8	0.0621
C_2	12.3	0.485
C_3	7.72	2.72
iC_4	1.04	1.23
nC_4	2.34	4.30
iC_5	0.533	2.45
nC_5	0.573	3.47
C_6	0.356	6.17
C_{7+}	4.50×10^{-5}	79.1

Table 5.4: Compositions of Sales Streams from Injected Gas Case in Mole %

utility from the three coolers is 2703 MBTU/h, and the total compression power is 778 hp. These additional power requirements represent a significant increase from the base case, which must be accounted for when determining the viability of the project.

Similar to the analysis performed in the IPR section, the effect of different tubing sizes was examined for the injected gas case. A range of diameters were set in the production tubing without changing any other variables in the process. This includes the split fraction, which remained at 80%, as the tubing diameter was incrementally changed from 1.0 to 4.0 in. The results of this analysis are presented in Figure 5.6, which shows a similar trend to the results of the base case analysis given in Figure 5.2. The main difference between the two cases is the lower plateauing pressure of the well fluid at larger diameters.

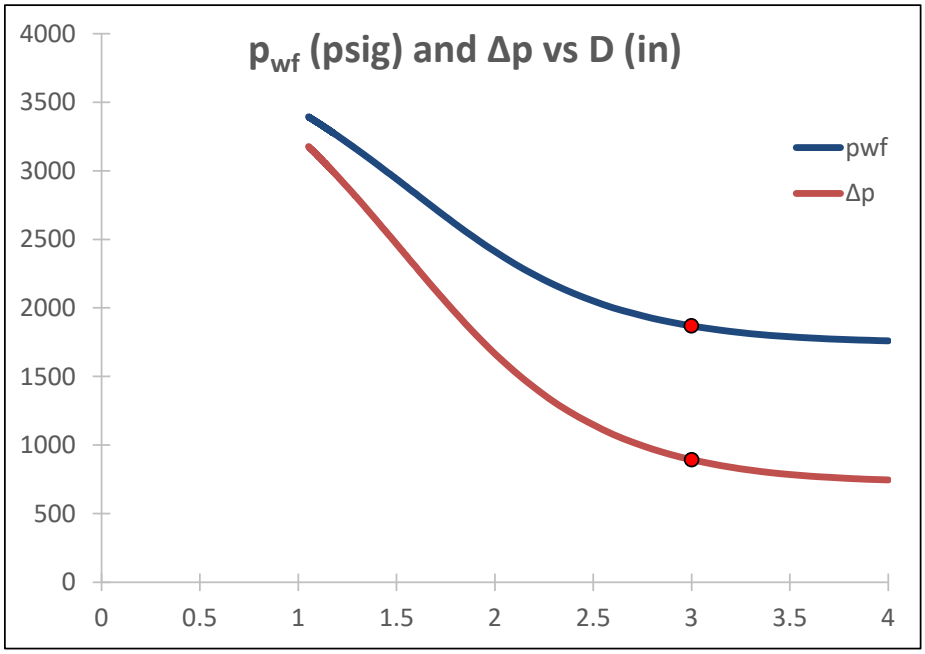

Figure 5.6: Recycle Case Well Fluid Pressure and Tubing Pressure Drop with Varying Tubing Diameter

In the base case, the well fluid pressure leveled off at about 2100 psig, and the pressure drop leveled off at close to 1230 psi. For the injected gas case, the well fluid pressure reached a low of 1760 psig, and the pressure drop decreased down to 750 psi. The lower well fluid pressures and tubing pressure drops at larger diameters in the recycle case are a result of lower fluid density with the addition of lift gas. The lower well fluid pressure also increases production rate according to the IPR. For this reason, a graph of the produced oil vs tubing size for the recycle case would take a similar form to the graph given in Figure 5.3 with slightly larger production rates at larger diameters. As before, both the well fluid pressure and the pressure drop in the tubing will approach the reservoir pressure at lower tubing diameters until the two curves intersect.

The impact the tubing diameter has on the system can be extended to another dimension with the addition of the recycle fraction variable in the injected gas case. To determine the system response for both the tubing size and recycle fraction, the simulation was solved over a range of

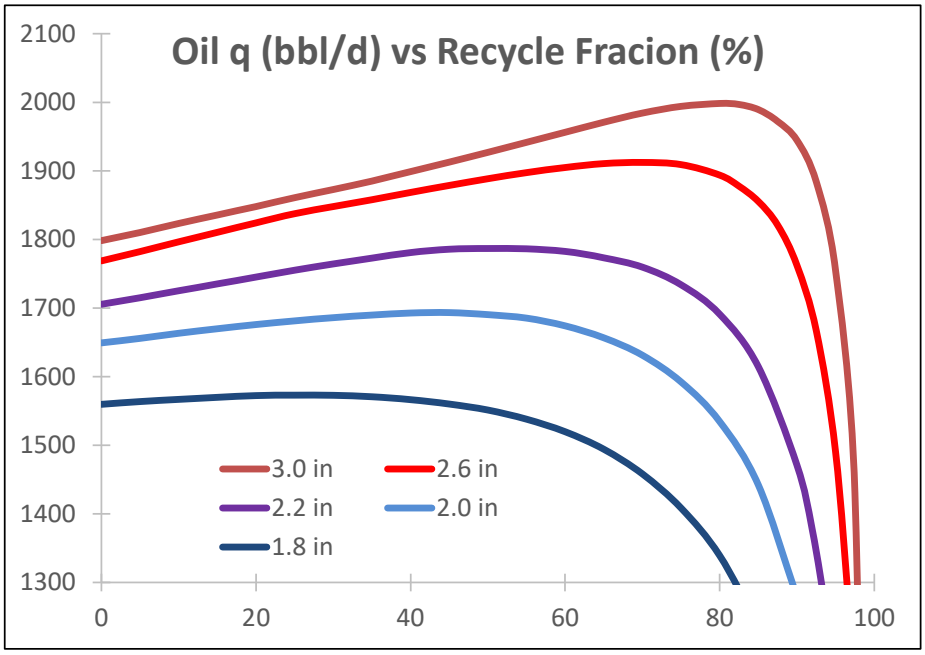

Figure 5.7: Oil Stock Tank Flow Rate as a Function of Tubing Size and Recycle Fraction

recycle fractions from 0 to 100% and over a range of tubing diameters. The collection of these data produces a series of production curves, each corresponding to a different tubing diameter, as a function of recycle fraction. Several of these production curves are given in Figure 5.7 with associated diameters of 3.0, 2.6, 2.2, 2.0, and 1.8 in.

Each curve begins at a split fraction of 0% which corresponds to the base case with no recycle gas. The curves increase before reaching a peak and rapidly decrease as the split fraction approaches 100%. A 100% split fraction corresponds to infinite recycle, with an infinite pressure drop, halting production. At sufficiently low tubing diameters, the addition of tubing gas does not increase production for any split fraction, meaning lift gas does not improve the system. The largest tubing diameter which does not benefit from recycle is about 1.6 in, and all curves below this diameter have a maximum production at 0% recycle. Figure 5.7 also shows a trend of increasing optimal split fraction with increasing tubing diameter. The optimal split fractions for the given curves, from smaller to larger diameter, are 80, 70, 50, 43, and 26%.

5.4 Economic and Sustainability Analysis

The economic analysis of the process seeks to determine, from a strictly financial perspective, if the addition of the gas lift project is viable. The project is incremental in nature, meaning the economic analysis will also be an incremental one, and many of the costs associated with the base process do not have to be considered. First, the cost of additional equipment to implement gas lift is estimated to establish an incremental capital investment for the project. These equipment costs are estimated using the six-tenths rule and a reference gas lift process. Table 5.5 gives data from the reference paper used to estimate the capital costs associated with gas lift.

Process	Gas Lift
Capital Cost ($MM)	0.53
Year	2018
CEPCI (January 2018)	576.4
Injected Gas Flow Rate (MMSCFD)	2.44

Table 5.5: Process Economic Data from Reference Paper (Hullio et al., 2018)

Using data from Table 5.5 and Equations 4.11 and 4.12, the cost of implementing gas lift for the examined system is estimated to be $0.844 MM. This capital cost is the fixed capital investment (FCI) for equipment, piping, and instrumentation. The total capital investment (TCI) is made up of the FCI and working capital investment (WCI), which is estimated to be a fraction of 15/85 of the FCI. The TCI can, therefore, be found as 100/85 of the FCI and equals $0.993 MM.

Next, the operating cost of implementing gas lift must be estimated before determining the incremental return on investment. No raw materials are required, as the injection gas is recycled from the well, so the operating costs consist of utility, maintenance, and labor costs. These costs

are estimated using the reference plant given above, and the results are given in Table 5.6. These expenses are not the total from the process, but the increased costs associated with injecting gas into the well.

Expense Type	**Cost ($MM)**
Utilities	1.11
Labor	1.10
Maintenance	0.947
Product Treatment and Transportation	0.868
Total	4.03

Table 5.6: Estimated Operating Expenses Associated with Gas Lift

The ROI is calculated using Equation 1.7, which requires the annual net economic profit (AEP). This profit is found using Equation 5.1 below with a tax rate of 30%. In the equation below, DFCI is the depreciated FCI which is found using Equation 5.2.

$$AEP = (Total\ Revenue - Total\ Operating\ Cost - DFCI) \times (1 - Tax\ Rate) + DFCI \tag{5.1}$$

$$DFCI = \frac{FCI - FCI_s}{n} \tag{5.2}$$

In the DFCI equation, FCI_s is the salvage value of the capital investment, which is assumed to be zero, and n is the life of the equipment, which is taken to be 10 years in this case. Using these values and the FCI value calculated previously, the DFCI is estimated to be \$0.0844 MM. To

determine AEP, the annual revenue must first be found. The total revenue is the sum of both oil and gas revenue incremental from the base case, having no gas lift.

The addition of gas lift increases the oil production rate by 199.8 bbl/d and the gas rate by 111.9 MSCFD. The assumed prices for these two commodities are given in Table 4.3. The price of oil is adjusted from $61.11/bbl to $59.11/bbl to account for crude treatment costs. Using these two prices and incremental flow rates, the annual gross incremental revenue is $4.43 MM. This value is used in Equation 5.1 and gives an AEP of $0.302 MM and a corresponding ROI of 30.4%, using the TCI value of $0.993 MM found earlier. This incremental ROI demonstrates the financial viability of the project, as typical thresholds for a project ROI are 10 - 20%.

The ROI calculated above does not account for the increased emissions from the oil stock tank or the increase in CO_2 emissions which result from the increase in compression, heating, and cooling utilities. The impact the project has on these sustainability metrics is found by comparing the base case values to the case with gas lift, and both these metrics will be given weighting of 0.1 compared to the net profit. The base stock tank emissions are 41.8 MSCFD, compared to the injection case, which had a value of 50.9 MSCFD. The differences between the two cases, with respect to CO_2 emissions, are summarized in Table 5.7.

Unit	**Base Case (MTPA)**	**Recycle Case (MTPA)**
VRU Cooler	3.73	4.98
VRU Compressor	41.6	56.6
Heater Treater	146	368
Interstage Coolers	0	59.7
Injection Gas Compressors	0	3870
Total	192	4360

Table 5.7: Comparison of CO_2 Emissions from Process Units

The annual CO_2 emissions from the equipment in the base case and the injection gas case were calculated based on their energy requirements. The coolers for the VRU and between compression stages were assumed to be fin fan air coolers with a forced draft. The Gas Processors Suppliers Association (GPSA) Engineering Data Book provides a procedure with accompanying data tables and charts to approximate the brake horsepower of such an exchanger (GPSA, 2017). This procedure was followed to determine the power requirements of all coolers in the two cases. These power requirements, along with those of the compressors, were assumed to be met with diesel-powered combustion engines on site. The corresponding CO_2 emissions were estimated using Equation 5.3.

$$E_{CO_2} = \frac{P \times HR \times EF}{HC} \tag{5.3}$$

Where:

E_{CO_2} = CO_2 Emissions,

EF = Emissions Factor,

HC = Heat Content,

HR = Heat Rate,

P = Power

The annual emissions are found by converting the energy rate required to a heating duty using a heat rate factor of 7700 BTU/hph. This factor is also taken from the GPSA handbook for estimating engine performance. The heat rate of the engine is supplied by the heat content of diesel fuel, which is assumed to be 5.825 MMBTU/bbl, and the CO_2 emissions from this fuel is estimated using an emissions factor from the EPA of 429.61 kg CO_2/bbl diesel with complete combustion (EPA, 2018).

Next, the CO_2 emissions from the heater treater were estimated using a ProMax simulation to model the combustion of a small portion of the sales gas stream as fuel. The required duty, supplied by combustion, is equal to the duty of the heater treater found previously. The flow rate of fuel gas

was determined by this duty, the heat content of the fuel as calculated by the simulation, and an efficiency factor of 60% (Garg, 2010). The stoichiometric balance of air was fed to the combustion unit with 10% excess. Complete combustion was again assumed, and the CO_2 emissions were found from the flow rate and composition of the flue gas.

Both metrics of sustainability increased from the base case, with a 24% increase in stock tank emissions and a 22-fold increase in CO_2 emissions. These increases lead to a less-sustainable process, but, to quantify how much less sustainable, the parameters ASP and ISWROIM were found according to Equations 1.9 and 1.11. Weights of 0.1 for both metrics and target values equal to the base case values were used in the calculation. With these assumptions, the value of the annual sustainability profit is largely influenced by the increase in CO_2 emissions and is found to be -0.363. The ISWROIM is calculated from the ASP and TCI to give a value of -36.5% and indicates the project would have a largely negative impact on the sustainability of the overall process.

The dramatic difference between ROI and ISWROIM can be explained by the lack of utilities in the base case. The only units in the process with utility demands before gas lift is implemented are the heater treater, VRU compressor, and VRU cooler. Their energy requirements are dwarfed by the compression power required to inject gas back into the well. This situation is exacerbated by the high optimal recycle split fraction of 80%, which demands yet more compression and cooling utilities. A sensitivity analysis on the weight given to the CO_2 emissions metric finds a break-even point at 0.045. In other words, if the decision makers were to reduce the relative importance of the carbon footprint to 4.5% of the profitability of the project, then the project would have an ASP and ISWROIM of zero. Taken together, these factors indicate the increase in profitability of the process does not justify the dramatic increase in CO_2 emissions.

6. CONCLUSIONS

The addition of a gas lift project to a production well was examined in this study to determine the viability of the project with assumed operating conditions. The production well was initially modeled without lift gas to provide a baseline for comparison and to indicate the improvement provided by the project. Both cases were examined with the aid of process simulation software which evaluated the physical properties of streams at steady-state operating conditions. The lift gas was split from the product gas stream as a recycle and compressed for re-injection. The optimal split fraction was determined by successive simulation, and the fraction producing the largest flow rate of product oil was selected.

The economic viability of the project was established using an incremental return on investment calculation based on estimated revenue, operating expenses, and capital costs. The ROI for the project exceeds typical minimum acceptable thresholds and indicates the project would greatly increase the profitability of the overall process. However, with the addition of gas lift, a compression train is required to compress the recycled gas. The compression process and interstage cooling is energy-intensive and results in far more CO_2 emissions than the process would have otherwise. The project also requires a large recycle fraction, which increases the needed compression and subsequent emissions.

Oil stock tank emissions and CO_2 emissions were selected as metrics of sustainability for the incremental project. The target values for both these indicators were selected from the base case results, which had lower emissions. The incremental ASP and ISWROIM were found to greatly deteriorate from the purely economic evaluation of the project. Not only does the project fall short of a minimum acceptable threshold, it negatively impacts the sustainability weighted return of the overall process. This study demonstrates the importance of considering sustainability metrics when evaluating potential projects with promising economic returns.

REFERENCES

Alarcón, G. A., Torres, C. F., and Gómez, L. E. Global optimization of gas allocation to a group of wells in artificial lift using nonlinear constrained programming. *Journal of Energy Resources Technology*, 124(4):262–268, 2002. ISSN 0195-0738.

Beggs, H. D. *Production optimization : using NODAL analysis*. Petroskills Publications, 1991. ISBN 0930972147 9780930972141.

Brill, J. P. and Beggs, H. D. *Two-Phase Flow in Pipes*. University of Tulsa, 1991.

Brill, J. P. and Mukherjee, H. K. *Multiphase Flow in Wells*. Henry L Doherty Monograph Series. Society of Petroleum Engineers, Richardson, Texas, first printing. edition, 1999. ISBN 1555630804 9781555630805.

Brown, K. E. Overview of artificial lift systems. *Journal of Petroleum Technology*, 34(10):2384–2396, 1982. ISSN 0149-2136.

CEPCI. Economic indicators. *Chemical Engineering*, 127(4):68, 04 2020.

Darcy, H. *Les fontaines publiques de la ville de Dijon*. Dalmont, 1856.

Denney, D. Simulation and optimization of continuous gas lift. *Journal of Petroleum Technology*, 54(05):60–60, 2002. ISSN 0149-2136.

Dutta-Roy, K. and Kattapuram, J. A new approach to gas-lift allocation optimization. *Society of Petroleum Engineers*, 1997.

EIA. US energy facts explained, 2019. URL `https://www.eia.gov/energyexplained/us-energy-facts/`.

El-Halwagi, M. A shortcut approach to the multi-scale atomic targeting and design of cho symbiosis networks. *Process Integration and Optimization for Sustainability*, 2017.

EPA. Greenhouse gas inventory guidance: direct emissions from stationary combustion sources, 2016. URL `https://www.epa.gov/climateleadership`.

EPA. US annual national emission factor, year 2016 data, 2018. URL `https://www.epa.gov/energy/emissions-generation-resource-integrated-database-egrid`.

Fetkovich, M. J. The isochronal testing of oil wells. *48th Annual Fall Meeting of SPE*, 1973. ISSN 978-1-55563-773-6.

Garg, A. *A New Approach to Optimizing Fired Heaters*. Energy Systems Laboratory Texas A&M University (http://esl.tamu.edu), 2010.

Gilbert, W. Flowing and gas-lift performance. *American Petroleum Institute*, 1954.

GPSA. *Engineering data book*. Gas Processors Suppliers Association, Tulsa, Okla., 14th edition, 2017.

Hullio, I., Jokhio, S., Memon, K., Nawab, S., and Baloch, K. Design and economic evaluation of the esp and gas lift on the dead oil well. *International Journal of Current Engineering and Technology*, 8, 2018.

Jones, L. G., Blount, E. M., and Glaze, O. H. Use of short term multiple rate flow tests to predict performance of wells having turbulence. *SPE Annual Fall Technical Conference and Exhibition*, 1976. ISSN 978-1-55563-744-6.

Kanu, E. P., Mach, J., and Brown, K. E. Economic approach to oil production and gas allocation in continuous gas lift (includes associated papers 10858 and 10865). *Journal of Petroleum Technology*, 33(10):1887–1892, 1981. ISSN 0149-2136.

Mahmudi, M. and Sadeghi, M. T. The optimization of continuous gas lift process using an integrated compositional model. *Journal of Petroleum Science and Engineering*, 108:321–327, 2013. ISSN 0920-4105.

Mora, O., Startzman, R. A., Saputelli, L., Ribeiro, L., Nunes, J. O. L., and Halliburton, E. Maximizing net present value in mature gas-lift fields. In *Proceedings of the SPE Hydrocarbon Economics and Evaluation Symposium: Hydrocarbon DevelopmentA Global Challenge*, pages 123–131, 2005.

Osuji, L. C. Review of advances in gas lift operations. *Society of Petroleum Engineers*, 1994.

Redden, J. D., Sherman, T. A. G., and Blann, J. R. Optimizing gas-lift systems. *Society of Petroleum Engineers*, 1974.

Satter, A. and Iqbal, G. M. *Reservoir engineering : the fundamentals, simulation, and management*

of conventional and unconventional recoveries. Gulf Professional Publishing, 2016. ISBN 9780128005231.

Towler, G. P. and Sinnott, R. K. *Chemical engineering design : principles, practice, and economics of plant and process design*. Butterworth-Heinemann, 2nd ed. edition, 2013. ISBN 9780080966595.

Vogel, J. V. Inflow performance relationships for solution-gas drive wells. *Journal of Petroleum Technology*, 20(01), 1968. ISSN 0149-2136.

Vázquez-Román, R. and Palafox, P. A new approach for continuous gas lift simulation and optimization. *Proceedings - SPE Annual Technical Conference and Exhibition*, 2005. ISSN 9781555631505.

Wang, X. and Economides, M. *Advanced Natural Gas Engineering*. Gulf Publishing Company, 2009. ISBN 978-1-933762-38-8.

APPENDIX A

SIMULATION RESULTS

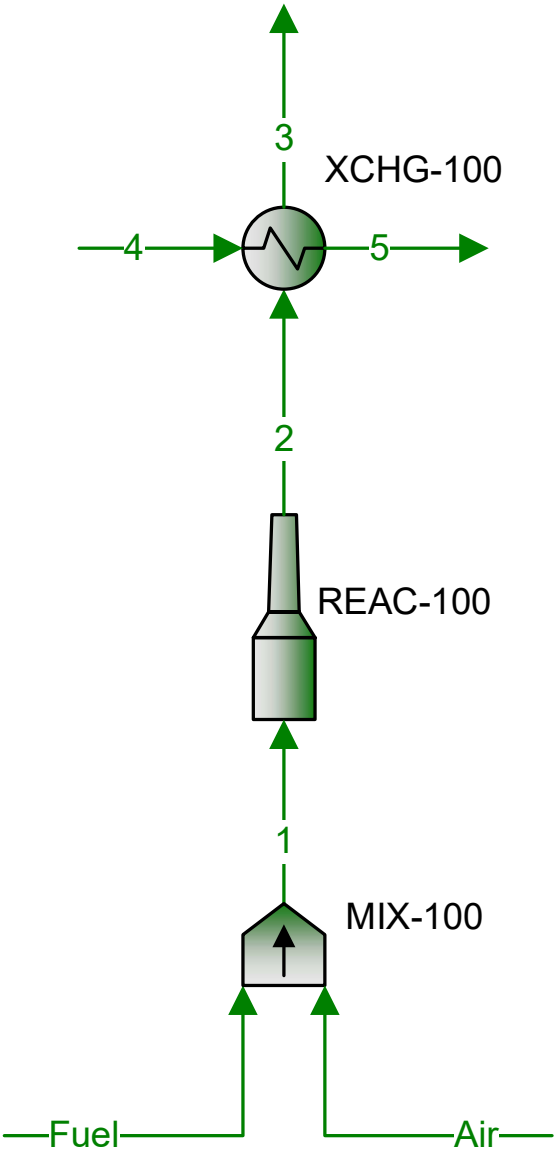

Figure A.1: Heater Treater Utility Flowsheet

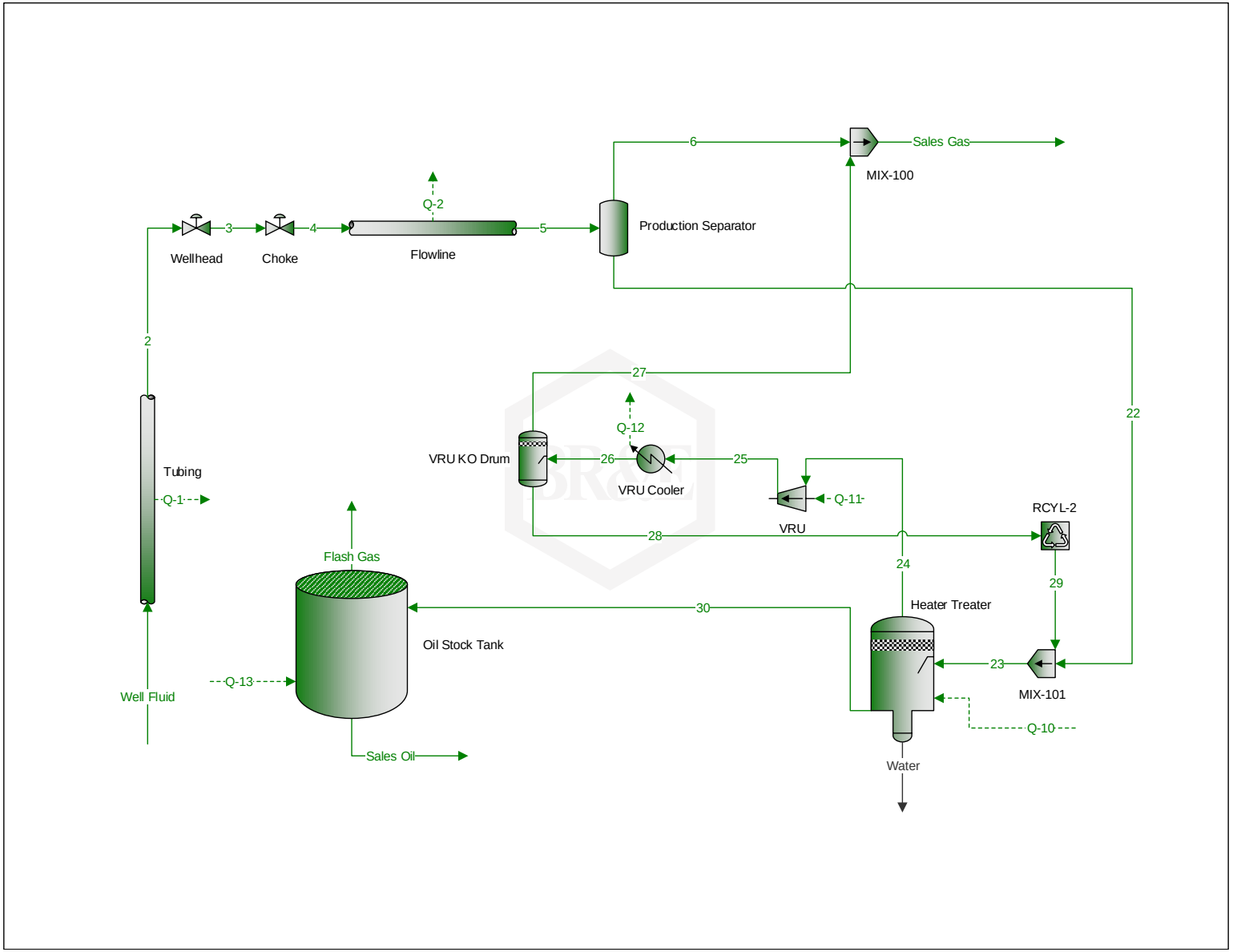

Figure A.2: ProMax Flowsheet of Well without Gas Lift

Process Streams		Flash Gas	Sales Gas	Sales Oil	Water	Well Fluid	2	3	4	5	6
Properties	Status:	Solved	Solved	Solved	Solved	Solved	Solved	Solved	Solved	Solved	Solved
Phase: Total	From Block:	Oil Stock Tank	MIX-100	Oil Stock Tank	Heater Treater	--	Tubing	Wellhead	Choke	Flowline	Production Separator
	To Block:	--	--	--	--	Tubing	Wellhead	Choke	Flowline	Production Separator	MIX-100
Property	Units										
Temperature	°F	100*	132.233	100	150	200*	157.076	157.078	147.698	133.778	133.778
Pressure	psia	14.6959*	214.696	14.6959	64.6959	2124.73*	892.941	893.211*	223.045	214.696	214.696*
Mole Fraction Vapor	%	100	100	0		17.2958	35.3947	35.3896	49.9983	49.3743	100
Molecular Weight	lb/lbmol	42.2425	22.7982	210.944		107.527	107.527	107.527	107.527	107.527	22.0935
Mass Density	lb/ft^3	0.104756	0.806904	53.2127		39.6416	24.6872	24.6932	6.77076	6.76128	0.777097
Molar Flow	lbmol/h	4.59150	127.695	107.517	0	239.803	239.803	239.803	239.803	239.803	118.401
Mass Flow	lb/h	193.956	2911.20	22680.0	0	25785.2	25785.2	25785.2	25785.2	25785.2	2615.89
Std Vapor Volumetric Flow	MMSCFD	0.0418176	1.16299	0.979223	0	2.18403	2.18403	2.18403	2.18403	2.18403	1.07835
Std Liquid Volumetric Flow	Mbbl/d	0.0272443	0.547999	1.79851	0	2.37376*	2.37376	2.37376	2.37376	2.37376	0.500716
Enthalpy	MMBtu/h	-0.205801	-4.42159	-17.6119		-21.2104	-21.7597	-21.7597	-21.7597	-21.9416	-4.05382
Mass Enthalpy	Btu/lb	-1061.07	-1518.82	-776.539		-822.580	-843.883	-843.883	-843.883	-850.937	-1549.69

Process Streams		22	23	24	25	26	27	28	29	30
Properties	Status:	Solved	Solved	Solved	Solved	Solved	Solved	Solved	Solved	Solved
Phase: Total	From Block:	Production Separator	MIX-101	Heater Treater	VRU	VRU Cooler	VRU KO Drum	VRU KO Drum	RCYL-1	Heater Treater
	To Block:	MIX-101	Heater Treater	VRU	VRU Cooler	VRU KO Drum	MIX-100	RCYL-1	MIX-101	Oil Stock Tank
Property	Units									
Temperature	°F	133.778	133.778	150*	298.893	120*	120	120	120	150
Pressure	psia	214.696	214.696	64.6959*	219.696*	214.696	214.696	214.696	214.696	64.6959
Mole Fraction Vapor	%	0	0	100	100	99.9694	100	0	0	0
Molecular Weight	lb/lbmol	190.848	190.845	31.7864	31.7864	31.7864	31.7759	66.0917	66.0917	204.035
Mass Density	lb/ft^3	51.7838	51.7837	0.322590	0.894669	1.22232	1.22157	36.2574	36.2574	51.6923
Molar Flow	lbmol/h	121.402	121.405	9.29644	9.29644	9.29644	9.29359	0.00284618	0.00284619	112.108
Mass Flow	lb/h	23169.3	23169.5	295.500	295.500	295.500	295.312	0.188109	0.188110	22874.0
Std Vapor Volumetric Flow	MMSCFD	1.10568	1.10571	0.0846684	0.0846684	0.0846684	0.0846425	2.59219E-05	2.59220E-05	1.02104
Std Liquid Volumetric Flow	Mbbl/d	1.87304	1.87306	0.0473042	0.0473042	0.0473042	0.0472829	2.13107E-05	2.13108E-05	1.82576
Enthalpy	MMBtu/h	-17.8878	-17.8880	-0.361348	-0.340070	-0.367962	-0.367768	-0.000194022	-0.000194023	-17.3167
Mass Enthalpy	Btu/lb	-772.046	-772.048	-1222.83	-1150.83	-1245.22	-1245.35	-1031.43	-1031.43	-757.049

Table A.1: Stream Properties for the Base Case Simulation

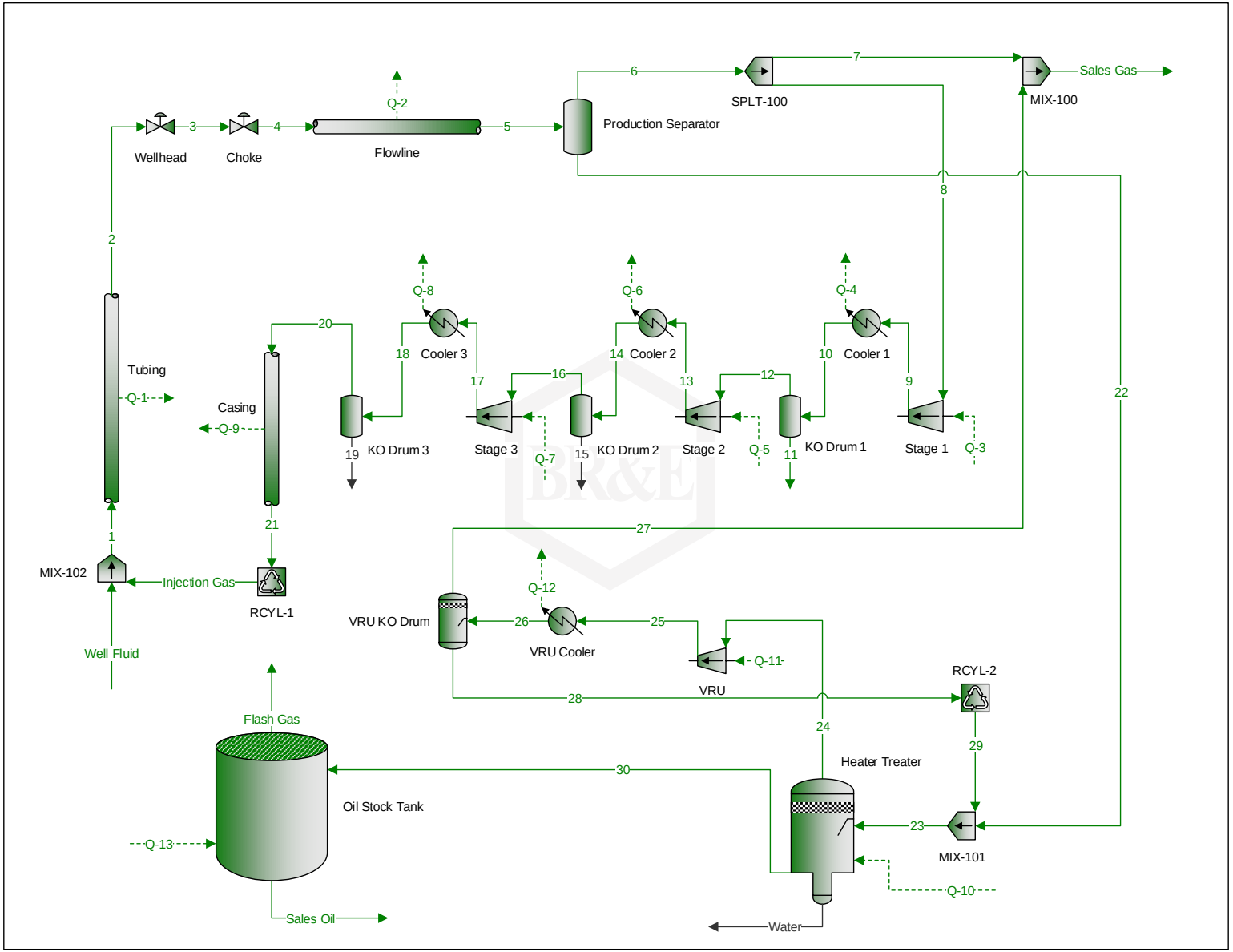

Figure A.3: ProMax Flowsheet of Well with Gas Lift

Process Streams		Flash Gas	Injection Gas	Sales Gas	Sales Oil	Water	Well Fluid	1	2	3
Properties	Status:	Solved	Solved	Solved	Solved	Solved	Solved	Solved	Solved	Solved
Phase: Total	From Block:	Oil Stock Tank	RCYL-1	MIX-100	Oil Stock Tank	Heater Treater	--	MIX-102	Tubing	Wellhead
	To Block:	--	MIX-102	--	--	--	MIX-102	Tubing	Wellhead	Choke
Property	Units									
Temperature	°F	100*	135.671	113.453	100	150	200*	179.492	144.143	144.142
Pressure	psia	14.6959*	1884.02	214.696	14.6959	64.6959	1883.43*	1883.43	989.385	989.320*
Mole Fraction Vapor	%	100	100	100	0		21.5994	70.1667	74.7757	74.7762
Molecular Weight	lb/lbmol	43.0921	21.4297	22.4324	209.898		107.527	50.9456	50.9456	50.9456
Mass Density	lb/ft^3	0.106921	8.19715	0.823138	53.1698		37.2839	17.4097	10.2693	10.2686
Molar Flow	lbmol/h	5.59380	509.158	139.983	119.943	0	265.605	774.763	774.763	774.763
Mass Flow	lb/h	241.049	10911.1	3140.16	25175.7	0	28559.6	39470.7	39470.7	39470.7
Std Vapor Volumetric Flow	MMSCFD	0.0509462	4.63721	1.27491	1.09239	0	2.41903	7.05625	7.05625	7.05625
Std Liquid Volumetric Flow	Mbbl/d	0.0335395	2.12589	0.596868	1.99833	0	2.62917*	4.75506	4.75506	4.75506
Enthalpy	MMBtu/h	-0.253179	-17.8641	-4.84926	-19.5656		-23.4919	-41.3559	-41.8552	-41.8552
Mass Enthalpy	Btu/lb	-1050.32	-1637.24	-1544.27	-777.162		-822.555	-1047.76	-1060.41	-1060.41

Process Streams		4	5	6	7	8	9	10	11	12
Properties	Status:	Solved	Solved	Solved	Solved	Solved	Solved	Solved	Solved	Solved
Phase: Total	From Block:	Choke	Flowline	Production Separator	SPLT-100	SPLT-100	Stage 1	Cooler 1	KO Drum 1	KO Drum 1
	To Block:	Flowline	Production Separator	SPLT-100	MIX-100	Stage 1	Cooler 1	KO Drum 1	--	Stage 2
Property	Units									
Temperature	°F	121.464	112.939	112.939	112.939	112.939	242.345	120*	120	120
Pressure	psia	268.444	214.696	214.696*	214.696	214.696	470.397	465.397	465.397	465.397
Mole Fraction Vapor	%	81.6571	82.1611	100	100	100	100	100		100
Molecular Weight	lb/lbmol	50.9456	50.9456	21.4314	21.4314	21.4314	21.4314	21.4314		21.4314
Mass Density	lb/ft^3	2.73370	2.20383	0.783351	0.783351	0.783351	1.39640	1.76067		1.76067
Molar Flow	lbmol/h	774.763	774.763	636.554	127.311	509.243	509.243	509.243	0	509.243
Mass Flow	lb/h	39470.7	39470.7	13642.2	2728.45	10913.8	10913.8	10913.8	0	10913.8
Std Vapor Volumetric Flow	MMSCFD	7.05625	7.05625	5.79749	1.15950	4.63799	4.63799	4.63799	0	4.63799
Std Liquid Volumetric Flow	Mbbl/d	4.75506	4.75506	2.65791	0.531581	2.12632	2.12632	2.12632	0	2.12632
Enthalpy	MMBtu/h	-41.8552	-41.9751	-21.7167	-4.34334	-17.3733	-16.6843	-17.4376		-17.4376
Mass Enthalpy	Btu/lb	-1060.41	-1063.45	-1591.87	-1591.87	-1591.87	-1528.73	-1597.76		-1597.76

Table A.2: Stream Properties for the Recycle Case Simulation (1/2)

Process Streams		13	14	15	16	17	18	19	20	21
Properties	Status:	Solved	Solved	Solved	Solved	Solved	Solved	Solved	Solved	Solved
Phase: Total	From Block:	Stage 2	Cooler 2	KO Drum 2	KO Drum 2	Stage 3	Cooler 3	KO Drum 3	KO Drum 3	Casing
	To Block:	Cooler 2	KO Drum 2	--	Stage 3	Cooler 3	KO Drum 3	--	Casing	RCYL-1
Property	Units									
Temperature	°F	251.767	120*	120	120	249.910	120*	120	120	135.663
Pressure	psia	1019.68	1014.68	1014.68	1014.68	2223.14	2218.14	2218.14	2218.14*	1883.97
Mole Fraction Vapor	%	100	100		100	100	100		100	100
Molecular Weight	lb/lbmol	21.4314	21.4314		21.4314	21.4314	21.4314		21.4314	21.4314
Mass Density	lb/ft^3	3.08972	4.25661		4.25661	6.98059	10.3377		10.3377	8.19833
Molar Flow	lbmol/h	509.243	509.243	0	509.243	509.243	509.243	0	509.243	509.243
Mass Flow	lb/h	10913.8	10913.8	0	10913.8	10913.8	10913.8	0	10913.8	10913.8
Std Vapor Volumetric Flow	MMSCFD	4.63799	4.63799	0	4.63799	4.63799	4.63799	0	4.63799	4.63799
Std Liquid Volumetric Flow	Mbbl/d	2.12632	2.12632	0	2.12632	2.12632	2.12632	0	2.12632	2.12632
Enthalpy	MMBtu/h	-16.7687	-17.6697		-17.6697	-17.0476	-18.0966		-18.0966	-17.8677
Mass Enthalpy	Btu/lb	-1536.47	-1619.02		-1619.02	-1562.03	-1658.14		-1658.14	-1637.17

Process Streams		22	23	24	25	26	27	28	29	30
Properties	Status:	Solved	Solved	Solved	Solved	Solved	Solved	Solved	Solved	Solved
Phase: Total	From Block:	Production Separator	MIX-101	Heater Treater	VRU	VRU Cooler	VRU KO Drum	VRU KO Drum	RCYL-2	Heater Treater
	To Block:	MIX-101	Heater Treater	VRU	VRU Cooler	VRU KO Drum	MIX-100	RCYL-2	MIX-101	Oil Stock Tank
Property	Units									
Temperature	°F	112.939	112.941	150*	295.923	120*	120	120	120	150
Pressure	psia	214.696	214.696	64.6959*	219.696*	214.696	214.696	214.696	214.696	64.6959
Mole Fraction Vapor	%	0	0	100	100	99.6947	100	0	0	0
Molecular Weight	lb/lbmol	186.880	186.845	32.5801	32.5801	32.5801	32.4888	62.3860	62.3860	202.465
Mass Density	lb/ft^3	52.1959	52.1941	0.331121	0.923727	1.26358	1.25646	35.1599	35.1599	51.6236
Molar Flow	lbmol/h	138.209	138.248	12.7113	12.7113	12.7113	12.6725	0.0388039	0.0388019	125.537
Mass Flow	lb/h	25828.5	25830.9	414.134	414.134	414.134	411.713	2.42082	2.42070	25416.8
Std Vapor Volumetric Flow	MMSCFD	1.25876	1.25911	0.115769	0.115769	0.115769	0.115416	0.000353411	0.000353393	1.14334
Std Liquid Volumetric Flow	Mbbl/d	2.09716	2.09744	0.0655678	0.0655678	0.0655678	0.0652865	0.000281309	0.000281295	2.03187
Enthalpy	MMBtu/h	-20.2584	-20.2610	-0.498845	-0.469877	-0.508470	-0.505922	-0.00254823	-0.00254810	-19.2657
Mass Enthalpy	Btu/lb	-784.344	-784.369	-1204.55	-1134.60	-1227.79	-1228.82	-1052.63	-1052.63	-757.990

Table A.3: Stream Properties for the Recycle Case Simulation (2/2)

APPENDIX B

CALCULATIONS

	Oil (bbl)	Gas (MMSCF)
Base q (per day)	1799	1.163
Recycle q (per day)	1998	1.275
Δq (per day)	199.8	0.112
Yearly (per year)	72934	40.85
Price ($)	59.11	2860
ΔSales ($/yr)	4311146	116833
Total ($MM/yr)	4.428	

Table B.1: Incremental Revenue Calculations

Compressor	Power (hp)	Per Annum (hph)	Heat (MMBTU)	Fuel (bbl)	Emissions (MTPA CO2)
Base VRU	8.36	73256	564	97	42
Recycle VRU	11.38	99729	768	132	56636
Stage1 Cooler	270.82	2372388	18267	3136	1347271
Stage2 Cooler	262.88	2302831	17732	3044	1307770
Stage3 Cooler	244.46	2141504	16490	2831	1216153
Interstage Coolers	12.00	105120	809	139	59697
VRU Cooler Recycle	1.00	8760	67	12	4975
VRU Cooler Base	0.75	6570	51	9	3731

Heat Rate (MMBTU/hph)
0.0077
Heat Content (MMBTU/bbl)
5.825
Emissions (kg CO2 /bbl)
429.61

Table B.2: Utility Calculations